Gas-Phase Non-Identity S_N2 Reactions of Halide Anions with Methyl Halides: A High-Level Computational Study

Mikhail N. Glukhovtsev,[1a,b] Addy Pross,*[,1a,c] and Leo Radom*[,1d]

Contribution from the School of Chemistry, University of Sydney, Sydney, NSW 2006, Australia, Department of Chemistry, Ben-Gurion University of the Negev, Beer Sheva 84105, Israel, and Research School of Chemistry, Australian National University, Canberra, ACT 0200, Australia

Received October 31, 1995. Revised Manuscript Received April 26, 1996[⊗]

Abstract: High-level ab initio molecular orbital calculations at the G2(+) level of theory have been carried out for the six non-identity nucleophilic substitution reactions, $Y^- + CH_3X \rightarrow YCH_3 + X^-$, for Y, X = F, Cl, Br, and I. Central barrier heights ($\Delta H^{\ddagger}_{cent}$) for reaction in the exothermic direction vary from 0.8 kJ mol^{-1} for Y = F, X = I up to 39.5 kJ mol^{-1} for Y = Cl, X = Br (at 0 K), and are in most cases significantly lower than those for the set of identity S_N2 reactions $X^- + CH_3X \rightarrow XCH_3 + X^-$ (X = F−I). Overall barriers ($\Delta H^{\ddagger}_{ovr}$) for reaction in the exothermic direction are all negative (varying from −68.9 kJ mol^{-1} for Y = F, X = I to −2.3 kJ mol^{-1} for Y = Br, X = I), in contrast to the overall barriers for the identity reactions where only the value for X = F is negative. Complexation enthalpies (ΔH_{comp}) of the ion−molecule complexes $Y^-\cdots CH_3X$ vary from 30.4 kJ mol^{-1} for Y = F, X = I to 69.6 kJ mol^{-1} for Y = I, X = F (at 298 K), in good agreement with experimental and earlier computational studies. Complexation enthalpies in the reaction series $Y^- + CH_3X$ (Y = F−I, X = F, Cl, Br, I) are found to exhibit good linear correlations with halogen electronegativity. Both the central barriers and the overall barriers show good linear correlations with reaction exothermicity, indicating a rate−equilibrium relationship in the $Y^- + CH_3X$ reaction set. The data for the central barriers show good agreement with the predictions of the Marcus equation, though modifications of the Marcus equation that consider overall barriers are found to be less satisfactory. Further interesting features of the non-identity reaction set are the good correlations between the central barriers and the geometric looseness (%$L^{\ddagger}$), geometric asymmetry (%AS), charge asymmetry (Δq(X−Y)), and bond asymmetry (ΔWBI) of the transition structures.

Introduction

Bimolecular nucleophilic substitution (S_N2) reactions at saturated carbon in the gas phase

$$X^- + CH_3X \rightarrow XCH_3 + X^- \text{ (X = F, Cl, Br, and I)} \quad (1)$$

$$Y^- + CH_3X \rightarrow YCH_3 + X^- \text{ (Y, X = F, Cl, Br, and I)} \quad (2)$$

have attracted considerable interest, both experimentally[2,3] and theoretically,[2,4−11] because of their fundamental nature. Yet despite this great interest, it is remarkable that considerable uncertainty still exists regarding the barrier heights for these reactions. On the one hand, due to the limitations of current experimental techniques, direct experimental data are available only for very few reactions and even here the results have been the subject of continuing debate.[2a,3b,k] On the other hand, the computational data have been found to be very sensitive to the level of theory employed so that theory also has not been a definitive source of information.

The possible effect of reaction dynamics in gas-phase S_N2 reactions,[4ab,5,11−13] and their influence on the interpretation of the experimental data, has recently been discussed. Most experimental kinetic data on gas-phase S_N2 reactions have been interpreted and rationalized[3kp,14−16] within models based on statistical theories, in particular Rice−Ramsperger−Kassel−Marcus (RRKM) theory[17] or phase space theory.[16] Assuming that ion−molecule complexes are long-lived and their internal energy distributed statistically, RRKM theory has been widely used to calculate the rate constants for ion−molecule complexes crossing over the central barrier or dissociating back into reactants. However, experimental data[3de,16,18] and theoretical trajectory calculations[4a,11,19] have recently provided evidence for non-statistical behavior in gas-phase S_N2 reactions 1 and 2 (particularly for the groups H, OH, F, Cl, and Br) so that the RRKM model may give rise to incorrect estimates of the reaction rate constants and, therefore, of barrier heights. At

⊗ Abstract published in *Advance ACS Abstracts,* June 15, 1996.

(1) (a) University of Sydney. (b) Present address: Department of Chemistry, Wayne State University, Detroit, Michigan 48202. (c) Ben-Gurion University of the Negev. (d) Australian National University.

(2) Comprehensive collections of both experimental and computational data up to 1991 may be found in the monographs: (a) Shaik, S. S.; Schlegel, H. B.; Wolfe, S. *Theoretical Aspects of Physical Organic Chemistry, The S_N2 Mechanism*; Wiley: New York, 1992. (b) Minkin, V. I.; Simkin, B. Y.; Minyaev, R. M. *Quantum Chemistry of Organic Compounds—Mechanisms of Reactions*; Springer Verlag: Berlin, 1990.

(3) Recent papers include the following: (a) Van Doren, J. M.; DePuy, C. H.; Bierbaum, V. M. *J. Phys. Chem.* **1989**, *93*, 1130. (b) DePuy, C. H.; Gronert, S.; Mullin, A.; Bierbaum, V. M. *J. Am. Chem. Soc.* **1990**, *112*, 8650. (c) Gronert, S.; DePuy, C. H.; Bierbaum, V. M. *J. Am. Chem. Soc.* **1991**, *113*, 4009. (d) VanOrden, S. L.; Pope, R. M.; Buckner, S. W. *Organic Mass Spectrom.* **1991**, *26*, 1003. (e) Graul, S. T.; Bowers, M. T. *J. Am. Chem. Soc.* **1991**, *113*, 9696. (f) Cyr, D. M.; Posey, L. A.; Bishea, G. A.; Han, C.-C.; Johnson, M. A. *J. Am. Chem. Soc.* **1991**, *113*, 9697. (g) Wladkowski, B. D.; Lim, K. F.; Allen, W. D.; Brauman, J. I. *J. Am. Chem. Soc.* **1992**, *114*, 9136. (h) Cyr, D. M.; Bishea, G. A.; Scarton, M. G.; Johnson, M. A. *J. Chem. Phys.* **1992**, *97*, 5911. (i) Wilbur, J. L.; Wladkowski, B. D.; Brauman, J. I. *J. Am. Chem. Soc.* **1993**, *115*, 10823. (j) Knighton, W. B.; Bognar, J. A.; O'Connor, P. M.; Grimsrud, E. P. *J. Am. Chem. Soc.* **1993**, *115*, 12079. (k) Wladkowski, B. D.; Brauman, J. I. *J. Phys. Chem.* **1993**, *97*, 13158. (l) Giles, K.; Grimsrud, E. P. *J. Phys. Chem.* **1993**, *97*, 1318. (m) Cyr, D. M.; Scarton, G.; Johnson, M. A. *J. Chem. Phys.* **1993**, *99*, 4869. (n) Strode, K. S.; Grimsrud, E. P. *Int. J. Mass Spectrom. Ion Processes* **1994**, *130*, 227. (o) Viggiano, A. A.; Morris, R. A.; Su, T.; Wladkowski, B. D.; Craig, S. L.; Zhong, M.; Brauman, J. I. *J. Am. Chem. Soc.* **1994**, *116*, 2213. (p) Wladkowski, B. D.; Wilbur, J. L.; Brauman, J. I. *J. Am. Chem. Soc.* **1994**, *116*, 2471. (q) Morris, R. A.; Viggiano, A. A. *J. Phys. Chem.* **1994**, *98*, 3740. (r) Viggiano, A. A.; Paschkewitz, J. S.; Morris, R. A.; Paulson, J. F.; Gonzalez-Lafont, A.; Truhlar, D. G. *J. Am. Chem. Soc.* **1991**, *113*, 9404.

S0002-7863(95)03665-1 CCC: $12.00

the present time the generality of these non-statistical effects and their importance in S_N2 reactions remains an open question.[3k,16]

We have recently studied[9] the identity methyl-transfer reactions (eq 1) using a modification of G2 theory termed G2(+) theory. At this level of theory, the results appear to agree with the limited available experimental data and suggest (to the extent that the selected experimental data are themselves reliable) that meaningful barrier heights can be obtained computationally. That study led to the surprising conclusion that central barrier heights for the reaction $X^- + CH_3X$ vary only slightly (over a range of just 13.0 kJ mol^{-1} for X = F−I), and that only for X = F is there a negative overall barrier. We now extend our G2(+) study to non-identity methyl-transfer reactions (eq 2). The present work represents the first uniform computational study of this fundamental reaction for all the halogens at such a high level and will hopefully provide more reliable energy parameters. We use the results to assess the role of reaction thermodynamics in governing barrier heights and thereby test the applicability of Marcus theory[20,21] and the additivity postulate for intrinsic energies, as applied to gas-phase S_N2 halide-exchange reactions.[3k] In addition, this data set may be useful for further dynamics modeling studies that consider non-statistical effects.

Computational Methods

It is clear from the very large number of calculations already carried out on S_N2 reactions at carbon[2,4−11] that the computational data are very sensitive to the level of theory employed. For this reason, in our earlier study of identity S_N2 halide-exchange reactions at carbon,[9] we used a level of theory, specifically a modification of G2 theory,[22] that is higher than the levels[4−8,10,11] used previously in comparative studies, and which appeared to be able to reproduce quite well the (albeit limited) experimentally available data. In the present study, we apply this same level of theory to the set of non-identity reactions.

Standard ab initio molecular orbital calculations[23] were carried out using a modified form of G2 theory[22] with the GAUSSIAN 92 system of programs.[24] G2 theory corresponds effectively to calculations at the QCISD(T)/6-311+G(3df,2p) level with zero-point vibrational energy (ZPE) and higher level corrections. It has been shown[22,25,26] to perform well for the calculation of atomization energies, ionization energies, electron affinities, bond energies, proton affinities, acidities, and reaction barriers.

Our modifications to G2 theory have been introduced to allow a better description of anions and for computational simplification. In the first place, geometries are optimized and vibrational frequencies determined with a basis set that includes diffuse functions, specifically

(4) Recent papers include the following: (a) Vande Linde, S. R.; Hase, W. L. *J. Phys. Chem.* **1990**, *94*, 2778. (b) Vande Linde, S. R.; Hase, W. L. *J. Phys. Chem.* **1990**, *94*, 6148. (c) Wolfe, S.; Kim, C.-K. *J. Am. Chem. Soc.* **1991**, *113*, 8056. (d) Zhao, X. G.; Tucker, S. C.; Truhlar, D. G. *J. Am. Chem. Soc.* **1991**, *113*, 826. (e) Kabbaj, O. K.; Lepetit, M. B.; Malrieu, J. P.; Sini, G.; Hiberty, P. C. *J. Am. Chem. Soc.* **1991**, *113*, 5619. (f) Gronert, S. *J. Am. Chem. Soc.* **1991**, *113*, 6041. (g) Shi, Z.; Boyd, R. J. *J. Am. Chem. Soc.* **1991**, *113*, 1072. (h) Jensen, F. *Chem. Phys. Lett.* **1992**, *196*, 368. (i) Sini, G.; Shaik, S.; Hiberty, P. C. *J. Chem. Soc., Perkin Trans. 2* **1992**, 1019 (j) Shi, Z.; Boyd, R. *Can. J. Chem.* **1992**, *70*, 450. (k) Barnes, J. A.; Williams, I. H. *J. Chem. Soc., Chem. Commun.* **1993**, 1286. (l) Gronert, S. *J. Am. Chem. Soc.* **1993**, *115*, 652. (m) Bickelhaupt, F. M.; Baerends, E. J.; Nibbering, N. M. M.; Ziegler, T. *J. Am. Chem. Soc.* **1993**, *115*, 9160. (n) Boyd, R. J.; Kim, C-K.; Shi, Z.; Weinberg, N.; Wolfe, S. *J. Am. Chem. Soc.* **1993**, *115*, 10147. (o) Shaik, S.; Ioffe, A.; Reddy, A. C.; Pross, A. *J. Am. Chem. Soc.* **1994**, *116*, 262. (p) Hu, W.-P.; Truhlar, D. G. *J. Phys. Chem.* **1994**, *98*, 1049. (q) Anh, N. T.; Maurel, F.; Thanh, B. T.; Thao, H. H.; N'Guessan, Y. T. *New J. Chem.* **1994**, *18*, 473. (r) Hu, W.-P.; Truhlar, D. G. *J. Am. Chem. Soc.* **1994**, *116*, 7797. (s) Shaik, S.; Reddy, A. C. *J. Chem. Soc., Faraday Trans.* **1994**, *90*, 1631. (t) Zahradnik, R. *Acc. Chem. Res.* **1995**, *28*, 306.

(5) Basilevsky, M. V.; Koldobskii, S. G.; Tikhomirov, V. A. *Russ. Chem. Rev.* (*Engl. Transl.*) **1986**, *55*, 948.

(6) (a) Shi, Z.; Boyd, R. J. *J. Am. Chem. Soc.* **1989**, *111*, 1575. (b) Shi, Z.; Boyd, R. J. *J. Am. Chem. Soc.* **1990**, *112*, 6789. (c) Shi, Z.; Boyd, R. J. *J. Am. Chem. Soc.* **1991**, *113*, 2434.

(7) Hu, W.-P.; Truhlar, D. G. *J. Am. Chem. Soc.* **1995**, *117*, 10726.

(8) Poirier, R.; Wang, Y.; Westway, K. C. *J. Am. Chem. Soc.* **1994**, *116*, 2526.

(9) Glukhovtsev, M. N.; Pross, A.; Radom, L. *J. Am. Chem. Soc.* **1995**, *117*, 2024.

(10) Hirao, K.; Kebarle, P. *Can. J. Chem.* **1989**, *67*, 1261.

(11) (a) Wang, H.; Zhu, L.; Hase, W. L. *J. Phys. Chem.* **1994**, *98*, 1608. (b) Wang, H.; Peslherbe, G. H.; Hase, W. L. *J. Am. Chem. Soc.* **1994**, *116*, 9644.

(12) (a) Truhlar, D. G.; Steckler, R.; Gordon, M. S. *Chem. Rev.* **1987**, *87*, 217. (b) Friedrich, B.; Herman, Z.; Zahradnik, R.; Havlas, Z. *Adv. Quantum. Chem.* **1988**, *19*, 247. (c) Truhlar, D. G.; Gordon, M. S. *Science*, **1990**, *249*, 491.

(13) Tucker, S. C.; Truhlar, D. G. *J. Phys. Chem.* **1989**, *93*, 8138.

(14) (a) Olmstead, W. N.; Brauman, J. I. *J. Am. Chem. Soc.* **1977**, *99*, 4219. (b) Pellerite, M. J.; Brauman, J. I. *J. Am. Chem. Soc.* **1980**, *102*, 5993. (c) Pellerite, M. J.; Brauman, J. I. *J. Am. Chem. Soc.* **1983**, *105*, 2672. (d) Pellerite, M. J.; Brauman, J. I. In *Mechanistic Aspects of Inorganic Reactions*; Rorabacher, D. R., Endicott, J. F., Eds.; ACS Symposium Series; American Chemical Society: Washington, DC, 1982; Vol. 198, p 81. (e) Barfknecht, A. T.; Dodd, J. A.; Salomon, K. E.; Tumas, W.; Brauman, J. I. *Pure Appl. Chem.* **1984**, *56*, 1809.

(15) (a) Dodd, J. A.; Brauman, J. I. *J. Am. Chem. Soc.* **1984**, *106*, 5356. (b) Dodd, J. A.; Brauman, J. I. *J. Phys. Chem.* **1986**, *90*, 3559.

(16) Graul, S. T.; Bowers, M. T. *J. Am. Chem. Soc.* **1994**, *116*, 3875.

(17) See, for example: (a) Gilbert, R. G.; Smith, S. C. *Theory of Unimolecular and Recombination Reactions*; Blackwell Scientific Publications: Oxford, 1990. (b) Forst, W. *Theory of Unimolecular Reactions*; Academic Press: New York, 1973. (c) Robinson, P. J.; Holbrook, K. A. *Unimolecular Reactions*; Wiley-Interscience: New York, 1972. (d) Pechukas, P. In *Dynamics of Molecular Collisions*, Part B; Miller, W. H., Ed.; Academic Press: New York, 1976. (e) Chesnavich, W. J.; Bowers, M. T. In *Gas Phase Ion Chemistry*; Bowers, M. T., Ed.; Academic Press: New York, 1979.

(18) Viggiano, A. A.; Morris, R. A.; Paschkewitz, J. S.; Paulson, J. F. *J. Am. Chem. Soc.* **1992**, *114*, 10477.

(19) (a) Vande Linde, S. R. V.; Hase, W. L. *J. Am. Chem. Soc.* **1989**, *111*, 2349. (b) Vande Linde, S. R. V.; Hase, W. L. *J. Chem. Phys.* **1990**, *93*, 7962. (c) Cho, Y. J.; Vande Linde, S. R.; Hase, W. L. *J. Chem. Phys.* **1992**, *96*, 8275.

(20) (a) Marcus, R. A. *J. Phys. Chem.* **1968**, *72*, 891. For further applications of Marcus theory to methyl-transfer reactions, see: (b) Lewis, E. S.; Hu, D. D. *J. Am. Chem. Soc.* **1984**, *106*, 3292. (c) Lewis, E. S.; Douglas, T. A.; McLaughlin, M. L. *Isr. J. Chem.* **1985**, *26*, 331. (d) Lewis, E. S. *J. Am. Chem. Soc.* **1986**, *90*, 3756.

(21) (a) Marcus, R. A. *Annu. Rev. Phys. Chem.* **1964**, *15*, 155. (b) Pross, A. *Theoretical and Physical Principles of Organic Reactivity;* Wiley: New York, 1995.

(22) Curtiss, L. A.; Raghavachari, K.; Trucks, G. W.; Pople, J. A. *J. Chem. Phys.* **1991**, *94*, 7221.

(23) Hehre, W. J.; Radom, L.; Schleyer, P. v. R.; Pople, J. A. *Ab Initio Molecular Orbital Theory;* Wiley: New York, 1986.

(24) Frisch, M. J.; Trucks, G. W.; Head-Gordon, M.; Gill, P. M. W.; Wong, M. W.; Foresman, J. B.; Johnson, B. G.; Schlegel, H. B.; Robb, M. A.; Replogle, E. S.; Gomperts, R.; Andres, J. L.; Raghavachari, K.; Binkley, J. S.; Gonzalez, C.; Martin, R. L.; Fox, D. J.; DeFrees, D. J.; Baker, J.; Stewart, J. J. P.; Pople, J. A. GAUSSIAN-92; Gaussian Inc.: Pittsburgh, PA, 1992.

(25) See, for example (a) Smith, B. J.; Radom, L. *J. Phys. Chem.* **1991**, 95, 10549. (b) Ma, N. L.; Smith, B. J.; Pople, J. A.; Radom, L. *J. Am. Chem. Soc.* **1991**, *113*, 7903. (c) Nobes, R. H.; Radom, L. *Chem. Phys. Lett.* **1992**, *189*, 554. (d) Yu, D.; Rauk, A.; Armstrong, D. A. *J. Phys. Chem.* **1992**, *96*, 6031. (e) Wong, M. W.; Radom, L. *J. Am. Chem. Soc.* **1993**, *115*, 1507. (f) Smith, B. J.; Radom, L. *J. Am. Chem. Soc.* **1993**, *115*, 4885. (g) Schlegel, H. B.; Skancke, A. *J. Am. Chem. Soc.* **1993**, *115*, 7465. (h) Goldberg, N.; Hrusák, J.; Iraqi, M.; Schwarz, H. *J. Phys. Chem.* **1993**, *97*, 10687. (i) Armstrong, D. A.; Rauk, A.; Yu, D. *J. Am. Chem. Soc.* **1993**, *115*, 666. (j) Wiberg, K.; Rablen, P. R. *J. Am. Chem. Soc.* **1993**, *115*, 9234. (k) Wiberg, K.; Nakaji, D. *J. Am. Chem. Soc.* **1993**, *115*, 10658. (l) Su, M.-D.; Schlegel, H. B. *J. Phys. Chem.* **1993**, *97*, 8732. (m) Darling, C. L.; Schlegel, H. B. *J. Phys. Chem.* **1993**, *97*, 1368. (n) Su, M.-D.; Schlegel, H. B. *J. Phys. Chem.* **1993**, *97*, 9981. (o) Lammertsma, K.; Prasad, B. V. *J. Am. Chem. Soc.* **1994**, *116*, 642. (p) Gauld, J. W.; Radom, L. *J. Phys. Chem.* **1994**, *98*, 777. (q) Chiu, S.-W.; Li, W.-K.; Tzeng, W-B.; Ng C-Y. *J. Chem. Phys.* **1992**, *97*, 6557. (r) Durant, J. L.; Rohlfing, C. M. *J. Chem. Phys.* **1993**, *98*, 8031. (s) Glukhovtsev, M. N.; Pross, A.; Radom, L. *J. Am. Chem. Soc.* **1994**, *116*, 5961. (t) Glukhovtsev, M. N.; Szulejko, J. E.; McMahon, T. B.; Gauld, J. G.; Scott, A. P.; Smith, B. J.; Pross, A.; Radom, L. *J. Phys. Chem.* **1994**, *98*, 13099.

(26) For a recent review, see: Curtiss, L. A.; Raghavachari, K. In *Quantum Mechanical Electronic Structure Calculations with Chemical Accuracy*; Langhoff, S. R., Ed.; Kluwer Academic Publishers: Amsterdam, 1995.

6-31+G(d) in place of 6-31G(d) for first- and second-row atoms. In addition, the MP2/6-31+G(d) optimizations are carried out with the frozen-core approximation rather than with all electrons being included in the correlation treatment. Finally, harmonic vibrational frequencies are calculated at the HF/6-31+G(d) level rather than HF/6-31G(d). This level of theory is termed G2(+). We note that geometry optimizations in some of the previous comparative studies have been performed at higher levels of theory than the MP2/6-31+G(d) level used here.[4r,7] However, the energy comparisons were carried out at levels lower than QCISD(T)/6-311+G(3df,2p).

For bromine- and iodine-containing species, our G2(+) calculations were carried out with the use of the effective core potentials (ECP) developed by Hay and Wadt.[27] Full details of the basis sets and procedures used are presented elsewhere.[28] Note that we have recommended[28] alternative ECP basis sets for bromine and iodine for use in *standard G2(ECP*) calculations.

Geometries were optimized using analytical gradient techniques.[29] The eigenvalue following method[30] was employed for transition structure optimizations. The stationary points on the potential energy surfaces were characterized by calculations of vibrational frequencies, which were carried out analytically for Y, X = F and Cl and numerically in ECP calculations of species containing Br and I.

Charge distributions were obtained from the wave functions calculated at the MP2/6-311+G(3df,2p) level on MP2/6-31+G(d) geometries, employing natural population analysis (NPA).[31,32]

In order to obtain enthalpies for the various species involved in reaction 2 at 298 K, enthalpy temperature corrections were derived using the harmonic frequencies computed at HF/6-31+G(d) and scaled by 0.8929,[22] and standard statistical thermodynamics formulas.[23] In the case of the $F^- + CH_3I$ reaction, the central barrier exists only at the MP2 level (see below), so the vibrational frequencies were calculated at MP2/6-31+G(d) and a scaling factor[33] of 0.9427 was used to calculate the zero-point vibration energies and the vibrational contributions to thermal corrections. Unless otherwise stated, we have used the results of G2(+) all electron (AE) calculations for F- and Cl-containing molecules and G2(+)-ECP calculations for Br- and I-containing molecules in our analysis. Throughout this paper, relative energies are presented as enthalpy changes (ΔH) at 0 and/or 298 K. Bond lengths are in angstroms and bond angles in degrees. Calculated total energies for all species involved in the non-identity reactions of Y^- and CH_3X may be found in the supporting information (Table S1).

Results and Discussion

The energy profile for an exothermic non-identity S_N2 reaction (eq 2) in the gas phase may be represented by an asymmetric double-well potential,[15,34] as shown in Figure 1. The reaction involves the initial formation of a pre-reaction ion−molecule complex, **1**, with a complexation enthalpy, ΔH_{comp},

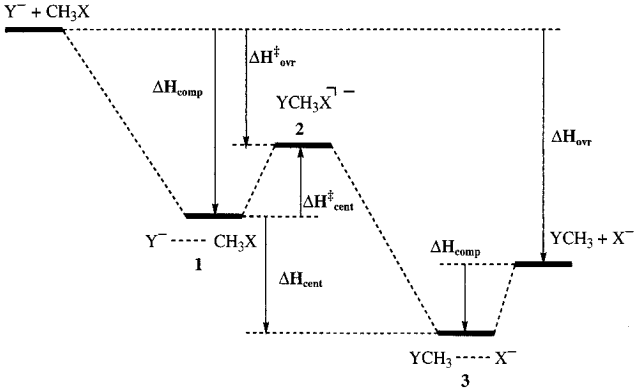

Figure 1. Schematic energy profile for the $Y^- + CH_3X$ non-identity exchange reaction (Y, X = F−I).

relative to separated reactants, which then must overcome an activation barrier that we term the *central* barrier, $\Delta H^{\ddagger}_{cent}$, to reach the transition structure, **2**. The energy then drops as the product ion−molecule complex, **3**, is produced and the latter can finally dissociate into separated products.[35] The *overall* activation barrier relative to separated reactants (as opposed to complex **1**) is denoted $\Delta H^{\ddagger}_{ovr}$. The *overall* enthalpy change in the reaction is denoted ΔH_{ovr} while the *central* enthalpy difference between product and reactant ion−molecule complexes **3** and **1** is denoted ΔH_{cent}. The existence of pre- and post-reaction complexes has recently been established experimentally for the systems $Cl^- + CH_3Br$[3e] and $I^- + CH_3Br$.[3h]

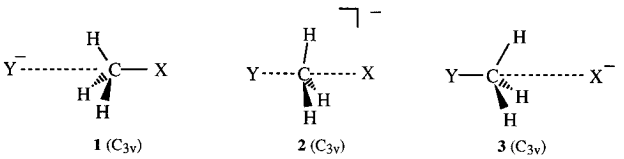

(**a**: Y = F, X = Cl; **b**: Y = F, X = Br; **c**: Y= F, X = I; **d**: Y= Cl, X = Br; **e**: Y = Cl, X = I; **f**: Y = Br, X = I)

A. CH_3X Structures (X = F, Cl, Br, and I). Calculated CH_3X geometries and NPA charge distributions were presented in our previous paper.[9] Geometries were found to be in reasonable agreement with experiment. The computational data indicated that the fluorine atom in CH_3F bears considerable negative charge, in contrast to the other CH_3X molecules where chlorine and bromine have near-zero charges, while iodine actually bears a positive charge.[9]

B. Ion−Molecule Complexes. As we discussed previously,[9] there are various conceivable geometries for these complexes.

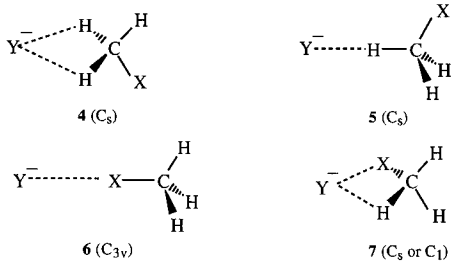

(27) Wadt, W. R.; Hay, P. J. *J. Chem. Phys.* **1985**, *82*, 284.
(28) Glukhovtsev, M. N.; Pross, A.; McGrath, M. P.; Radom, L. *J. Chem. Phys.* **1995**, *103*, 1878.
(29) (a) Schlegel, H. B. *J. Comput. Chem.* **1982**, *3*, 214. (b) Schlegel, H. B. In *Ab Initio Methods in Quantum Chemistry;* Lawley, K. P., Ed.; Wiley: New York, 1987; p 249.
(30) (a) Simons, J.; Jørgensen, P.; Taylor, H.; Ozment, J. *J. Phys. Chem.* **1983**, *87*, 2745. (b) Taylor, H.; Simons, J. *J. Phys. Chem.* **1985**, *89*, 684. (c) Baker, J. *J. Comput. Chem.* **1986**, *7*, 385. For a recent review, see: (d) McKee, M. L.; Page, M. In *Reviews in Computational Chemistry;* Lipkowitz, K. B., Boyd, D. B., Eds.; VCH: New York, 1993; Vol. 4; p 35.
(31) (a) Reed, A. R.; Weinstock, R. B.; Weinhold, F. *J. Chem. Phys.* **1985**, *83*, 735. (b) Reed, A. E.; Curtiss, L. A.; Weinhold, F. *Chem. Rev.* **1988**, *88*, 899. (c) Weinhold, F.; Carpenter, J. E. In *The Structure of Small Molecules and Ions*; Naaman, R., Vager, Z., Eds.; Plenum Press: New York, 1988; p 227. (d) Reed, A. E.; Weinhold, F. *Is. J. Chem.* **1991**, *31*, 277.
(32) For recent NPA applications, see, e.g.: (a) Reed, A. E.; Schleyer, P. v. R. *J. Am. Chem. Soc.* **1990**, *112*, 1434. (b) Glukhovtsev, M. N.; Schleyer, P. v. R. *Chem. Phys. Lett.* **1992**, *198*, 547. (c) Mestres, J.; Duran, M.; Bertran, J. *Theor. Chim. Acta* **1994**, *88*, 325. (d) Nemukhin, A. V.; Grigorenko, B. L. *Chem. Phys. Lett.* **1995**, *233*, 627.
(33) Pople, J. A.; Scott, A. P.; Wong, M. W.; Radom, L. *Isr. J. Chem.* **1993**, *33*, 345.
(34) (a) Lieder, C. A.; Brauman, J. I. *J. Am. Chem. Soc.* **1974**, *96*, 4029. (b) Brauman, J. I.; Olmstead, W. N.; Lieder, C. A. *J. Am. Chem. Soc.* **1974**, *96*, 4030.
(35) Of course this reaction profile provides a *static* picture for reactions 1 and 2 which does not take into account the possible influence of *dynamic* effects. For example, as was computationally found by Basilevsky and Ryaboy[5,36] and confirmed in detailed trajectory calculations by Hase and co-workers,[4b] it is possible that some identity and non-identity S_N2 methyl-transfer reactions may proceed via a direct substitution mechanism without the intermediate formation of the reactant ion−molecule complex.
(36) (a) Basilevsky, M. V.; Ryaboy, V. M. *Chem. Phys. Lett.* **1986**, *129*, 71. (b) Ryaboy, V. M. *Chem. Phys. Lett.* **1989**, *159*, 371.

Table 1. Complexation Enthalpies (ΔH_{comp}) of the Ion−Molecule Complexes, **1** and **3**, Calculated at the G2(+) Level (kJ mol^{-1})[a]

	F^-	Cl^-	Br^-	I^-
CH_3F	57.1 (56.5)[b]	39.3 (39.3)[c]	34.5 (34.6)	30.4 (30.7)[d]
CH_3Cl	64.6 (64.4)	43.7 (44.0)[b]	38.6 (39.0)[b]	33.9 (34.4)
CH_3Br	68.9 (68.9)	45.9 (46.3)[b,e]	40.5 (41.1)[b]	35.7 (36.3)
CH_3I	69.6 (69.6)[d]	45.3 (45.8)[f]	40.0 (40.7)	35.3 (36.0)[b,d]

[a] Calculated enthalpies at 298 K, with 0 K values given in parentheses. [b] Very recent experimental values[43a] are 50.2 ($F^-\cdots CH_3F$), 43.5 ($Cl^-\cdots CH_3Cl$), 46.9 ($Br^-\cdots CH_3Br$), 38.9 ($I^-\cdots CH_3I$), 52.3 ($Cl^-\cdots CH_3Br$), and 45.6 ($Br^-\cdots CH_3Cl$) kJ mol^{-1}. [c] An experimental estimate[43b,c] is 48.1 ± 8.4 kJ mol^{-1}. [d] The G2(+) complexation enthalpies were calculated using the MP2/6-31+G(d) zero-point energies and harmonic frequencies, see text. [e] An experimental estimate[41] is 41.8 ± 4.2 kJ mol^{-1}. An earlier experimental value[42] is 45.6 ± 2.1 kJ mol^{-1}. [f] An experimental value[42] is 41.0 ± 0.8 kJ mol^{-1}.

Previous studies[37−39] have suggested that complexes in which the halide ion coordinates with both the carbon and the three hydrogens (**1**) are lower in energy than those in which the halide ion coordinates with just two hydrogens (**4**), or with just one hydrogen (**5**). A further possible structure, **6**, corresponds to the pre-reaction complex for the so-called X-philic reaction which results in nucleophilic attack at halogen.[40] For the F^- + CH_3I system, our calculations actually indicate that **6c** is 30.3 kJ mol^{-1} lower in enthalpy than **1c** at 0 K. However, the two possible halophilic reactions

$$CH_3I + F^- \rightarrow (CH_3{-}I{-}F)^- \rightarrow CH_3^{\bullet} + IF^{\bullet -} \qquad (3a)$$

$$CH_3I + F^- \rightarrow (CH_3{-}I{-}F)^- \rightarrow CH_3^- + IF \qquad (3b)$$

are strongly endothermic (by 110.0 and 291.1 kJ mol^{-1}, respectively, at the G2(+) level at 298 K), in contrast to the S_N2 substitution pathway (eq 2) which is strongly exothermic (by 178.1 kJ mol^{-1} at 298 K at the G2(+) level). Therefore, formation of **6** does not appear to lead to a viable reaction channel, and accordingly is not considered further. Complex **7**, which might correspond to a pre-reaction complex for front-side attack, is also not considered here.

1. Complexation Enthalpies. Calculated G2(+) complexation enthalpies (ΔH_{comp}, see Figure 1) are compared with available experimental data in Table 1. The theoretical results confirm the experimental observation that the complexation enthalpies for $Cl^-\cdots CH_3X$ complexes lie in a fairly narrow range. The calculated complexation enthalpy of $Cl^-\cdots CH_3Br$ (**1d**) at 298 K (45.9 kJ mol^{-1}) lies within the range of the experimental values of 41.8 ± 4.2,[41] 45.6 ± 2.1,[42] and 52.3 kJ mol^{-1}.[43a] The G2(+) complexation enthalpy of $Cl^-\cdots CH_3I$ (**1e**) (45.3 kJ mol^{-1} at 298 K) is in good agreement with the HPMS experimental value[42] of 41.0 ± 0.8 kJ mol^{-1}. G2(+) calculations on $Cl^-\cdots CH_3F$ (**3a**) lead to a complexation enthalpy of 39.3 kJ mol^{-1} (298 K), which almost falls within the experimental range of 48.1 ± 8.4 kJ mol^{-1} obtained from ion cyclotron resonance chloride-transfer equilibrium measurements.[43b,c] Finally, the G2(+) complexation energy for $Br^-\cdots CH_3Cl$ (**3d**) of 38.6 kJ mol^{-1} at 298 K may be compared with an experimental value of 45.6 kJ mol^{-1}.[43a]

Table 2. Geometries (MP2/6-31+G(d)) of Ion−Molecule Complexes $Y^-\cdots CH_3X$ (**1**) and $YCH_3\cdots X^-$ (**3**) (Y, X = F, Cl, Br, and I)

complexes **1**	r(Y···C), Å	r(C−X), Å	r(C−H), Å	∠HCX, deg
$F^-\cdots CH_3Cl$ (**1a**)	2.616	1.832	1.083	108.5
$F^-\cdots CH_3Br$ (**1b**)	2.528	2.028	1.081	106.8
$F^-\cdots CH_3I$ (**1c**)	2.478	2.231	1.081	106.1
$Cl^-\cdots CH_3Br$ (**1d**)	3.199	1.992	1.084	107.7
$Cl^-\cdots CH_3I$ (**1e**)	3.175	2.180	1.084	107.6
$Br^-\cdots CH_3I$ (**1f**)	3.367	2.175	1.085	107.7
complexes **3**	r(C···X), Å	r(Y−C), Å	r(C−H), Å	∠YCH, deg
$FCH_3\cdots Cl^-$ (**3a**)	3.255	1.438	1.086	108.0
$FCH_3\cdots Br^-$ (**3b**)	3.457	1.435	1.087	108.0
$FCH_3\cdots I^-$ (**3c**)	3.738	1.431	1.087	108.0
$ClCH_3\cdots Br^-$ (**3d**)	3.457	1.807	1.085	108.9
$ClCH_3\cdots I^-$ (**3e**)	3.741	1.803	1.086	108.9
$BrCH_3\cdots I^-$ (**3f**)	3.668	1.983	1.085	107.8

The set of G2(+) complexation enthalpies (Table 1) indicates that complexation enthalpies for $Y^-\cdots CH_3X$ depend primarily on the identity of Y^-, and only to a smaller extent on the identity of CH_3X, and tend to decrease in the following order: F^- > Cl^- > Br^- > I^-. Thus, the complexation enthalpies for F^- range between 57.1 and 69.6 kJ mol^{-1}, those for Cl^- range between 39.3 and 45.9 kJ mol^{-1}, those for Br^- range between 34.5 and 40.5 kJ mol^{-1}, while those for I^- range between 30.4 and 35.7 kJ mol^{-1} (Table 1). For a given CH_3X, the complexation enthalpy is found to correlate with the electronegativity[45] of Y (e.g., r^2 = 0.983 for CH_3Br and correlation coefficients are even greater for the other methyl halides). This observation is in agreement with our earlier finding[9] that the G2(+) complexation enthalpies for $X^-\cdots CH_3X$ (X = F, Cl, Br, and I) also decrease in the order F > Cl > Br > I and show a good linear correlation with electronegativity. The complexation enthalpy−electronegativity correlations may be found in the supporting information (Figure S1).

The pattern of complexation enthalpies for $Y^-\cdots CH_3X$ as a function of X shows the following ordering: CH_3F < CH_3Cl < $CH_3Br \approx CH_3I$. The fact that CH_3Br and CH_3I form the strongest complexes with a given halide ion signifies that ion−dipole interactions (which would favor CH_3F) do not dominate the complexation enthalpies, and suggests that methyl halide electron affinity and/or polarizability (which would favor CH_3I) contribute most significantly.

2. Geometries. Calculated geometries of complexes **1a−f** and **3a−f** are presented in Table 2. The geometries of the CH_3X moieties within the $Y^-\cdots CH_3X$ complexes differ only slightly from those in unperturbed CH_3X. The $Y^-\cdots C$ distances in $Y^-\cdots CH_3X$ complexes (Y = F, Cl and Br) are shorter than the upper limits for specific interactions (2.94, 3.45, and 3.52 Å, respectively), estimated[46] from the mean-statistical values of the

(37) Schlegel, H. B.; Mislow, K.; Bernardi, F.; Bottoni, A. *Theor. Chim. Acta* **1977**, *44*, 245.
(38) Mitchell, D. J. Ph.D. Thesis, Queen's University, Kingston, Canada, 1981.
(39) Cremer, D.; Kraka, E. *J. Phys. Chem.* **1986**, *90*, 33.
(40) Zefirov, N. S.; Makhon'kov, D. I. *Chem. Rev.* **1982**, *82*, 615.
(41) Caldwell, G.; Magnera, T. F.; Kebarle, P. *J. Am. Chem. Soc.* **1984**, *106*, 959.
(42) (a) Dougherty, R. C.; Roberts, J. D. *Org. Mass Spectrom.* **1974**, *8*, 81. (b) Dougherty, R. C.; Dalton, J.; Roberts, J. D. *Org. Mass Spectrom.* **1974**, *8*, 77.
(43) (a) McMahon, T. B. Private communication. (b) Larson, J. W.; McMahon, T. B. *J. Am. Chem. Soc.* **1984**, *106*, 517. (c) Larson, J. W.; McMahon, T. B. *J. Am. Chem. Soc.* **1985**, *107*, 766.
(44) Lias, S. G.; Bartmess, J. E.; Liebman, J. F.; Holmes, J. L.; Levin, R. D.; Mallard, W. G. *J. Phys. Chem. Ref. Data* **1988**, *17*, Suppl. 1.
(45) For a discussion of the current status of the electronegativity concept in chemistry and for leading references, see (a) Allen, L. C. *Int. J. Quantum. Chem.* **1994**, *49*, 253. (b) Allen, L. C. *J. Am. Chem. Soc.* **1989**, *111*, 9003.
(46) (a) Zefirov, Yu. V.; Zorkii, P. M. *Russ. Chem. Rev.* (*Engl. Transl.*) **1995**, *64*, 415. (b) Zefirov, Yu. V.; Porai-Koshits, M. A. *Zh. Strukt. Khim.* (*Engl. Transl*) **1980**, *21*, 150. (c) Zefirov, Yu. V.; Porai-Koshits, M. A. *Zh. Strukt. Khim.* (*Engl. Transl*) **1986**, *27*, 74. (d) VWRs were obtained from X-ray diffraction data on organic crystal structures (VWR(C) = 1.71 Å, VWR(F) = 1.40 Å, VWR(Cl) = 1.90 Å, VWR(Br) = 1.97 Å, VWR(I) = 2.14 Å). The expression $2(R_AR_B)^{1/2}$ is used to estimate interatomic distances for ordinary van der Waals interactions using VWRs of A and B atoms, respectively.[46a−c] The upper limit for specific interactions is approximated as $2(R_AR_B)^{1/2} - 0.15$ Å.[46c]

Table 3. Overall Reaction Enthalpies (ΔH_{ovr}), Central Enthalpy Differences between Reactant and Product Ion−Molecule Complexes (ΔH_{cent}), Overall Barrier Heights ($\Delta H^{\ddagger}_{ovr}$), and Central Barrier Heights ($\Delta H^{\ddagger}_{cent}$) for Exothermic $Y^- + CH_3X$ Reactions, Calculated at the G2(+) Level (kJ mol^{-1})[a]

Y, X		ΔH_{ovr}	ΔH_{cent}	$\Delta H^{\ddagger}_{ovr}$	$\Delta H^{\ddagger}_{cent}$
F, Cl	G2(+)	−127.8 (−127.5)	−102.5 (−102.4)	−54.7 (−52.5) [−52.8]	9.9 (11.9)
	exptl	−143 ± 3[b]			29 ± 5[c]
F, Br	G2(+)	−160.1 (−159.6)	−125.7 (−125.3)	−67.7 (−65.8) [−66.1]	1.2 (3.1)
	exptl	−173 ± 4[b]			
F, I	G2(+)	−178.1 (−177.5)[d]	−139.4 (−138.9)[d]	−70.9 (−68.9) [−69.2][d]	−1.3 (0.8)[d,e]
	exptl	−201.4 ± 3.9[b]			
Cl, Br	G2(+)	−32.3 (−32.1)	−25.0 (−24.8)	−8.4 (−6.8) [−6.5]	37.5 (39.5)
	exptl	−30 ± 3[b]		−7.5[f]	
				−10.5 ± 2.1[g]	
				−9.2[h]	
				−8.2 ± 1.4[i]	
				−5.4[j]	
Cl, I	G2(+)	−50.4 (−49.9)	−39.0 (−38.6)	−15.3 (−13.8) [−14.2]	30.0 (32.0)
	exptl	−58 ± 3[b]		−19.3 ± 1.9[i]	
				−11.3[j]	
Br, I	G2(+)	−18.0 (−17.9)	−13.7 (−13.5)	−3.5 (−2.3) [−2.0]	36.5 (38.4)
	exptl	−29 ± 4[b]		−10.6 ± 1.9[i]	
				−5.9[j]	

[a] Calculated enthalpies at 298 K, with 0 K values given in parentheses. Values in square brackets represent $\Delta H^{\ddagger}$ values at 0 K without zero-point vibrational energies, sometimes referred to as $\Delta V^{\ddagger}$.[7] [b] Calculated from data in ref 44. [c] From ref 14c. [d] Standard G2(+) theory was employed to obtain the overall reaction enthalpy (ΔH_{ovr}). However, ΔH_{cent}, $\Delta H^{\ddagger}_{ovr}$, and $\Delta H^{\ddagger}_{cent}$ were calculated using the MP2/6-31+G(d) zero-point energies and harmonic frequencies, see text. [e] The thermal corrections lead to the enthalpy of TS **2** dropping below that of the reactant complex **1**, i.e. the central barrier disappears. [f] From ref 3k. [g] From ref 41. [h] From ref 3j. [i] Overall barriers at 0 K obtained from modeling the bimolecular kinetics with statistical phase space theory from ref 16. [j] Values from ref 7, obtained by fitting to experimental rate constants.

corresponding van der Waals radii (VWR) of the halogens and carbon,[46d] reflecting the bonding interaction between Y^- and CH_3X. The calculated C···Br$^-$ distances in **3b** and **3d** are found to be equal (3.457 Å) and in agreement with the X-ray C···Br$^-$ distance of 3.457 Å in $(PhCOCH_2P^+Ph_3)Br^-$,[46a] while the calculated C···Br$^-$ distance in **1f** (3.367 Å) is smaller. A slight shortening of the C−H length and a slight decrease in ∠HCX (or HCY in **3**) relative to the values in isolated CH_3X (CH_3Y) molecules are characteristic features of the calculated geometries of the ion−molecule complexes **1** and **3**. For complexes with iodide anion, the I$^-$···C distances are slightly longer than the upper limit for specific interactions (3.67 Å), which is consistent with the generally smaller complexation enthalpies of I$^-$···CH_3X (Table 1).

C. Transition Structures and Barrier Heights. Previous theoretical[2b,5,37,47] and experimental[48,49] data indicate a preference for back-side attack in reaction 2, with front-side attack, involving the formation of a transition structure with four-electron three-center cyclic delocalization,[5] predicted to be associated with much higher barriers.[2b,5,37,47,50] We therefore only consider back-side attack here. G2(+) values for the central barriers ($\Delta H^{\ddagger}_{cent}$) and the overall barriers ($\Delta H^{\ddagger}_{ovr}$) are included in Table 3. The geometries and charge distributions of the C_{3v} transition structures (**2**) are presented in Tables 4−6.

1. Barriers. Calculated central barriers ($\Delta H^{\ddagger}_{cent}$) at 0 K range from 0.8 kJ mol^{-1} for the reaction $F^- + CH_3I$ up to 39.5 kJ mol^{-1} for the reaction $Cl^- + CH_3Br$ (Table 3). These non-identity central barriers are significantly lower than the central barriers for the identity methyl-transfer reactions (eq 1) reported previously,[9] a result that is expected since the identity reactions are thermoneutral (by definition), while the non-identity reactions are all expressed in the exothermic direction. The same pattern is found for the overall reaction barriers ($\Delta H^{\ddagger}_{ovr}$). Thus, for the identity set the overall reaction barrier ($\Delta H^{\ddagger}_{ovr}$) is negative only for X = F,[9] while for the non-identity set, $\Delta H^{\ddagger}_{ovr}$ is negative in all cases (Table 3).[51]

Table 4. Geometries (MP2/6-31+G(d)) of the YCH_3X^- Transition Structures (**2**, X, Y = F, Cl, Br, and I)

species	r(Y···C), Å	r(C···X), Å	r(C−H), Å	∠HCX, deg
F···CH_3···Cl$^-$ (**2a**)	2.016	2.142	1.073	95.6
F···CH_3···Br$^-$ (**2b**)	2.108	2.242	1.075	97.9
F···CH_3···I$^-$ (**2c**)	2.180	2.386	1.076	99.8
Cl···CH_3···Br$^-$ (**2d**)	2.371	2.430	1.073	91.4
Cl···CH_3···I$^-$ (**2e**)	2.413	2.586	1.074	92.7
Br···CH_3···I$^-$ (**2f**)	2.520	2.634	1.075	91.2

It is of interest to compare our theoretical results with available experimental data. The kinetics of gas-phase halide-exchange reactions have been studied intensively,[3,14−16,18,41,48,49,52,54] although only in the exothermic direction.[55] Nonetheless, there is only a limited amount of direct experimental data available for their barriers, specifically for the reactions $Cl^- + CH_3Br$ (which has been studied in most detail[3b−f,j,k,l,11b,14−16,18,41,52,54]) and $F^- + CH_3Cl$.[3d,14c,48] Our calculated G2(+) overall barrier for the reaction $Cl^- + CH_3Br$ ($\Delta H^{\ddagger}_{ovr}$ = −8.4 kJ mol^{-1} at 298 K) is close to experimental

(47) Anh, N. T.; Minot, C. *J. Am. Chem. Soc.* **1980**, *102*, 103.

(48) Su, T.; Morris, R. A.; Viggiano, A. A.; Paulson, J. F. *J. Phys. Chem.* **1990**, *94*, 8426.

(49) Riveros, J. M.; Jose, S. M.; Takashima, K. *Adv. Phys. Org. Chem.* **1985**, *21*, 197.

(50) Glukhovtsev, M. N.; Pross, A.; Schlegel, H. B.; Radom, L. To be published.

(51) Positive overall barriers for reactions 2 with Y = F, X = Cl; Y = F, X= Br; and Y = Cl, X = Br have been deduced[52] from flowing afterglow measurements.[53] Arrhenius activation energies were simply estimated from the Arrhenius equation by assuming the pre-exponential factor to be equal to the ADO (averaged dipole orientation) collision rate constant. Transformation of these activation energies[52] into $\Delta H^{\ddagger}_{ovr}$ enthalpies led to slightly positive or near-zero values, in contrast to later results obtained using the ICR method[3k,53] and with a pulsed electron beam high ion source pressure mass spectrometer.[41,53] However, the correctness of the earlier estimates[52] has been questioned.[49]

(52) Tanaka, K.; Mackay, G. I.; Payzani, J. D.; Bohme, D. K. *Can. J. Chem.* **1976**, *54*, 1643.

(53) For a description of the various experimental techniques that can be applied to study gas-phase ion−molecule reactions, see, for example: *Techniques for the Study of Ion−Molecule Reactions;* Farrar, J. M.; Saunders, W. H., Eds.; Wiley: New York, 1988.

(54) (a) Damrauer, R.; DePuy, C. H.; Bierbaum, V. M. *Organometallics* **1982**, *1*, 1553. (b) Bierbaum, V. M.; Grabowski, J. J.; DePuy, C. H. *J. Phys. Chem.* **1984**, *88*, 1389.

(55) The reaction efficiency in the endothermic direction would be too small for the reaction to be experimentally observable.[3k]

Table 5. Looseness and Asymmetry Indexes[a] of the YCH_3X^- Transition Structures (**2**, X, Y = F, Cl, Br, and I)[a]

species	%CX‡	%CY‡	%L‡	%AS‡	WBI(C−X)	WBI(C−Y)	ΔWBI
$F\cdots CH_3\cdots Cl^-$ (**2a**)	16.9	40.2	57.1	23.3	0.591	0.209	0.382
$F\cdots CH_3\cdots Br^-$ (**2b**)	10.6	46.9	57.5	36.4	0.668	0.209	0.459
$F\cdots CH_3\cdots I^-$ (**2c**)	6.7	52.3	59.3	45.4	0.728	0.173	0.555
$Cl\cdots CH_3\cdots Br^-$ (**2d**)	22.0	31.2	53.2	9.2	0.496	0.394	0.102
$Cl\cdots CH_3\cdots I^-$ (**2e**)	18.6	33.8	52.5	15.2	0.549	0.357	0.192
$Br\cdots CH_3\cdots I^-$ (**2f**)	21.1	48.2	48.2	6.0	0.503	0.412	0.091

[a] %CX‡, %CY‡, and %L‡ are defined in eqs 4a−c. %AS‡ was calculated with eq 5. WBI(C−X) and WBI(C−Y) are the Wiberg bond indexes[67] calculated on the basis of the natural atomic orbitals[31a,b] for the C−X and Y−C bonds, respectively, in transition structure **2**. ΔWBI is the difference between these WBI values, calculated at the MP2/6-311+G(3df,2p) level.

Table 6. NPA Charge Distributions for the YCH_3X^- Transition Structures (**2**, Y, X = F, Cl, Br, and I)[a]

species	q(Y)	q(X)	q(C)	q(H)	$q(CH_3)$[b]	Δq(X−Y)[c]
$F\cdots CH_3\cdots Cl^-$ (**2a**)	−0.858	−0.590	−0.088	0.179	0.448	0.268
$F\cdots CH_3\cdots Br^-$ (**2b**)	−0.825	−0.415	−0.355	0.198	0.240	0.410
$F\cdots CH_3\cdots I^-$ (**2c**)	−0.847	−0.313	−0.459	0.206	0.160	0.534
$Cl\cdots CH_3\cdots Br^-$ (**2d**)	−0.657	−0.564	−0.391	0.204	0.221	0.093
$Cl\cdots CH_3\cdots I^-$ (**2e**)	−0.677	−0.494	−0.448	0.206	0.171	0.183
$Br\cdots CH_3\cdots I^-$ (**2f**)	−0.615	−0.526	−0.483	0.208	0.141	0.089

[a] Calculated at the MP2/6-311+G(3df,2p) level. [b] The CH_3 group charge provides an estimate of the extent of the contribution of the VB triple-ion $X^-R^+X^-$ configuration, see text. [c] $\Delta q(X-Y) = q(X) - q(Y)$ is the difference between the NPA charges at X and Y, and is a measure of the asymmetry of the charge distribution in **2**, see text.

estimates of −7.5,[3k] −9.2,[41] and −10.5 kJ mol^{-1}.[3j,56] Our G2-(+) $\Delta H^{\ddagger}_{ovr}$ values are also reasonably close to barrier heights obtained[7] by fitting rate constants in the canonical unified statistical (CUS) model with experimental rate constants at 300 K,[3a,18] utilizing calculated frequency and moment of inertia information. The barriers determined in this way are −5.4 (Cl^- + CH_3Br), −11.3 (Cl^- + CH_3I), and −5.9 kJ mol^{-1} (Br^- + CH_3I). Finally, our G2(+) $\Delta H^{\ddagger}_{ovr}$ values are also in satisfactory agreement with barriers at 0 K determined from modeling the bimolecular kinetics with statistical phase-space theory for the reactions Cl^- + CH_3Br (−8.2 ± 1.4 kJ mol^{-1}) and Cl^- + CH_3I (−19.3 ± 1.9 kJ mol^{-1}), but in less good agreement with the value for Br^- + CH_3I (−10.6 ± 1.9 kJ mol^{-1}).[16] Modeling based on phase-space theory gives an overall barrier for the identity (Cl, Cl) reaction of 11.6 ± 1.0 kJ mol^{-1}, for which the corresponding G2(+) value[9] is 11.5 kJ mol^{-1}. It is possible that the good agreement may be partly fortuitous, given the recent suggestion that S_N2 reactions may show non-statistical effects. Non-statistical effects, to the extent that they are significant, could be expected to undermine the RRKM or phase-space theory procedures by which the experimental values are obtained. Alternatively, the good agreement between theory and experiment could be taken as vindicating the use of statistical theories to characterize gross features of the S_N2 potential energy surfaces, such as the reaction barriers.[16]

The G2(+) central barrier for the reaction F^- + CH_3Cl (9.9 kJ mol^{-1}) is some 19 kJ mol^{-1} lower than the experimental estimate (at 298 K) (Table 3).[14c] This large discrepancy may in part be due to non-statistical behavior, discussed above, which has been shown to occur in this reaction.[3d] However, this is just one possible reason for the large discrepancy and the question needs to be explored further.

Lower level calculations on the F^- + CH_3Cl reaction barrier show a wide variation in results and are of little help in resolving the uncertainty. Thus, the reaction was found to be barrier-free at HF/4−31G,[61] but a central barrier of 25.6 kJ mol^{-1} was calculated at MP2/6-31++G(d,p).[6] While the latter value happens to agree with the experimental estimate of 28.9 kJ mol^{-1}, this is not considered to be significant since S_N2 barriers calculated at the MP2 level tend to be overestimated.[9,62]

Do gas-phase S_N2 reactions without a central barrier exist? Given that increasing reaction exothermicity lowers the barrier height, it is conceivable that highly exothermic reactions may be barrier-free in this sense.[2a,61] The G2(+) calculated enthalpy change for the reaction F^- + CH_3I is found to be −178.1 kJ mol^{-1} at 298 K.[63] As this reaction is the most exothermic of the set of non-identity halide-exchange reactions, the likelihood of a barrier-free reaction would be greatest in this case. Indeed, our estimate of the height of the central barrier at the G2(+) level (0 K) is just 0.8 kJ mol^{-1} (Table 3). The inclusion of temperature corrections to 298 K, calculated from the MP2 harmonic frequencies, results in the disappearance of the barrier. Thus our conclusion is that the reaction F^- + CH_3I has little or no barrier.[65] The experimental rate constant for the reaction of F^- with CH_3I (as with other basic anionic nucleophiles) is found to be encounter controlled,[48,54,64] but this finding by itself does not prove a barrier-free process.

2. Geometries. The geometric looseness of C−X and C−Y bonds in the transition structures, %C−X‡ and %C−Y‡, and the composite transition structure looseness, %L‡, have been previously defined[2a,66] by eqs 4a−c:

(56) The value of −10.5 kJ mol^{-1} was obtained at 640 Torr of buffer gas pressure.[3j] However, there are significant high-pressure kinetics effects[4n,57] for reaction 2 (Y = Cl, X = Br)[3j,58] and the overall barrier at atmospheric pressure is slightly higher (i.e. smaller in absolute magnitude).

(57) Basilevsky, M. V.; Weinberg, N. N.; Zhulin, V. M. *J. Chem. Soc., Faraday Trans. 1* **1985**, *81*, 875.

(58) Giles, K.; Grimsrud, E. P. *J. Phys. Chem.* **1992**, *96*, 6680.

(59) Wladkowski, B. D.; Allen, W. D.; Brauman, J. I. *J. Phys. Chem.* **1994**, *98*, 13532.

(60) Barlow, S. E.; Van Doren, J. M.; Bierbaum, V. M. *J. Am. Chem. Soc.* **1988**, *110*, 7240.

(61) Wolfe, S. *Can. J. Chem.* **1984**, *62*, 1465.

(62) Cernusak, I.; Urban, M. *Collect. Czech. Chem. Commun.* **1988**, *53*, 2239.

(63) This value underestimates that obtained from experimental enthalpies of formation (−201.4 ± 3.9 kJ mol^{-1} at 298 K)[44] (Table 3) by about 23 kJ mol^{-1}. This difference between G2(+) theory and experiment is larger than normal (where there is generally agreement to within 10 kJ mol^{-1}).[22] It arises because of small differences between the theoretical and experimental values of the heats of formation for each of the components of the F^- + CH_3I reaction [F^- (7.3 kJ mol^{-1}), CH_3I (4.4 kJ mol^{-1}), FCH_3 (3.9 kJ mol^{-1}), and I^- (7.6 kJ mol^{-1})][9] that happen to all reinforce one another in this reaction, rather than to partially cancel out.

(64) O'Hair, R. A. J.; Davico, G. E.; Hacaloglu, J.; Dang, T. T.; DePuy, C. H.; Bierbaum, V. M. *J. Am. Chem. Soc.* **1994**, *116*, 3609.

(65) High-level calculations of the F^- + CH_3I reaction as well as of the more exothermic OH^- + CH_3I reaction are in progress: Glukhovtsev, M. N.; Pross, A.; Radom, L. To be published.

(66) Shaik, S. S.; Schlegel, H. B.; Wolfe, S. *J. Chem. Soc., Chem. Commun.* **1988**, 1322.

$$\%CX^{\ddagger} = 100(d^{\ddagger}_{C-X} - d^{comp}_{C-X})/d^{comp}_{C-X} \quad (4a)$$

$$\%CY^{\ddagger} = 100(d^{\ddagger}_{C-Y} - d^{comp}_{C-Y})/d^{comp}_{C-Y} \quad (4b)$$

$$\%L^{\ddagger} = \%CX^{\ddagger} + \%CY^{\ddagger} \quad (4c)$$

where $d^{\ddagger}_{C-X}$ and $d^{\ddagger}_{C-Y}$ are the C−X and C−Y bond lengths in transition structure **2**, and d^{comp}_{C-X} and d^{comp}_{C-Y} are C−X and C−Y bond lengths in the reactant and product ion−molecule complexes **1** and **3**, respectively.[2a,4c,n] The geometrical asymmetry (%AS‡) of the transition structure **2** is defined[2a] by:

$$\%AS^{\ddagger} = \%CY^{\ddagger} - \%CX^{\ddagger} \quad (5)$$

The Wiberg bond indexes (WBI)[67] of the Y−C and C−X bonds in **2**, as well as their difference (ΔWBI), provide an additional estimate of transition structure looseness and asymmetry of bonding. All these measures of transition structure looseness and asymmetry are presented in Table 5 and their correlations with some of the other properties related to reaction 2 are discussed below.

3. Charge Distributions. Charge distributions in **2** (Table 6) indicate a substantial positive charge on the CH_3 moiety in all cases. This presumably reflects a significant contribution of the triple-ion valence bond (VB) configuration, $Y^-R^+X^-$,[2a,4i,68,69] for all halogens, which is particularly pronounced for the system $F^- + CH_3Cl$. NPA halogen charges are found to be in reasonable agreement with Bader charges (AIM).[4g] For example, at the MP2/6-311+G(3df,2p) level, the NPA charges on F and Cl in **2a** are −0.858 and −0.590 while the AIM charges calculated at MP2/6-31++G(d,p) are −0.814 and −0.623, respectively.[4g]

The coefficient of the VB triple-ion configuration $Y^-R^+X^-$ in the transition state wave function can be estimated as $|q(CH_3)|^{1/2}$, where $|q(CH_3)|$ is the absolute magnitude of the CH_3 group charge (assuming that contributions of configurations YR^-X, $Y^-R^-X^+$, and $Y^+R^-X^-$ are negligible).[4o,s] For $F^- + CH_3Cl$, this coefficient is 0.669 at MP2/6-311+G(3df,2p) (Table 6). Use of MP2/6-31++G(d,p) Bader charges gives a similar value of 0.661.[4g] For the identity methyl-transfer reaction, as the halogen electronegativity decreases, the contribution of the triple-ion configuration $X^-R^+X^-$ to the transition state wave function (given by the square of the coefficient and therefore equal to $|q(CH_3)|$) decreases from 0.432 for X = F to just 0.098 for X = I at MP2/6-311+G(3df,2p).[9] However, for non-identity methyl-transfer reactions, the electronegativities of X and Y do not appear to be the sole determinant of the extent of the triple-ion contribution. Thus, while the $q(CH_3)$ group charge is largest for $F^- + CH_3Cl$, the $q(CH_3)$ charge in **2f** (Y = Br, X = I) is the second largest in magnitude (Table 6).

The asymmetry of the charge distributions in **2a**−**f** can be described by the difference between q(X) and q(Y) charges. Correlations of $q(CH_3)$ and Δq(X−Y) (= q(X) − q(Y)) values with various kinetic and thermodynamic parameters are discussed in the next section.

D. Correlations of Barrier Heights. There has been considerable discussion in the literature as to what factors might influence barrier heights in gas-phase S_N2 reactions,[2a,4gj,6,7,14,15,61,66,70−74] so we briefly consider our computational data in this context.

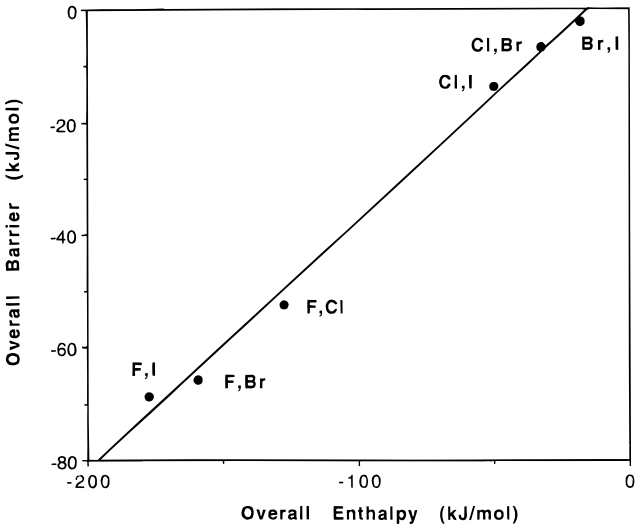

Figure 2. Plot of G2(+) overall barriers ($\Delta H^{\ddagger}_{ovr}$) vs G2(+) overall reaction enthalpies (ΔH_{ovr}) for the $Y^- + CH_3X$ non-identity exchange reactions (Y, X = F−I) at 0 K. $\Delta H^{\ddagger}_{ovr}$ and ΔH_{ovr} values are listed in Table 3.

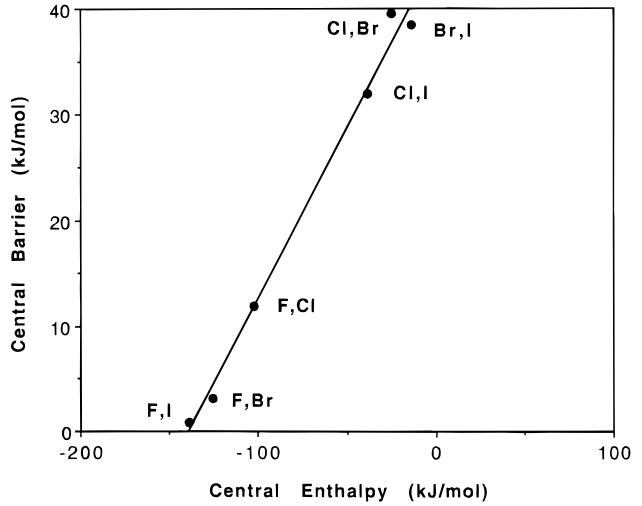

Figure 3. Plot of G2(+) central barriers ($\Delta H^{\ddagger}_{cent}$) vs G2(+) central enthalpies (ΔH_{cent}) for the $Y^- + CH_3X$ non-identity exchange reactions (Y, X = F−I) at 0 K. $\Delta H^{\ddagger}_{cent}$ and ΔH_{cent} values are listed in Table 3.

1. Rate−Equilibrium Relationship and Marcus Theory. By obtaining barrier heights and reaction enthalpies for a set of related reactions, it is possible to determine whether these reactions obey a rate−equilibrium relationship. A plot of the G2(+) overall barrier ($\Delta H^{\ddagger}_{ovr}$) versus the reaction enthalpy (ΔH_{ovr}) for the set of non-identity S_N2 reactions (eq 2) generates a good linear correlation (Figure 2; $r^2 = 0.995$). An analogous correlation is also found between the G2(+) central barriers ($\Delta H^{\ddagger}_{cent}$) and the central enthalpy change between product and reactant ion−molecule complexes, **3** and **1** (ΔH_{cent}) (Figure 3, $r^2 = 0.991$), as well as with the overall reaction enthalpy (ΔH_{ovr}) ($r^2 = 0.991$). The former correlation indicates that a barrier height−enthalpy correlation is also found for the elementary step for interconversion of reactant and product ion−molecule complexes. Thus, the reaction set obeys the Bell−Evans−Polanyi principle[75] and the empirical expression of Evans and

(67) Wiberg, K. B. *Tetrahedron* **1968**, *24*, 1083.
(68) (a) Dedieu, A.; Veillard, A. *J. Am. Chem. Soc.* **1972**, *94*, 6730. (b) Talaty, E. R.; Woods, J. J.; Simons, G. *Aust. J. Chem.* **1979**, *32*, 2289.
(69) Bader, R. F. W.; Duke, A. J.; Messer, R. R. *J. Am. Chem. Soc.* **1973**, *95*, 7715.
(70) Han, C.-C.; Dodd, J. A.; Brauman, J. I. *J. Phys. Chem.* **1986**, *90*, 471.
(71) Mitchell, D. J.; Schlegel, H. B.; Shaik, S. S.; Wolfe, S. *Can. J. Chem.* **1985**, *63*, 1642.
(72) (a) Shaik, S. S. *Isr. J. Chem.* **1985**, *26*, 367. (b) Shaik, S. S. *Can. J. Chem.* **1986**, *64*, 96. (c) Shaik, S. S. *Acta Chem. Scand.* **1990**, *44*, 205.
(73) Shaik, S. S. *J. Am. Chem. Soc.* **1988**, *110*, 1127.
(74) Wolfe, S.; Mitchell, D. J.; Schlegel, H. B. *J. Am. Chem. Soc.* **1981**, *103*, 7692.

Table 7. G2(+) Enthalpies of the Elementary Reaction Step (ΔH_{cent}),[a] Calculated Brønsted Coefficients α, Central ($\Delta H_o^{\ddagger}{}_{cent}$) and Overall ($\Delta H_o^{\ddagger}{}_{ovr}$) Intrinsic Barriers, and Estimated Central ($\Delta H^{\ddagger}{}_{cent}$) and Overall Barriers ($\Delta H^{\ddagger}{}_{ovr}$) (in kJ mol^{-1}) Using Various Forms of the Marcus Equation (at 0 K)

Y, X	G2(+) ΔH_{cent}[a]	α[b]	G2(+) $\Delta H_0^{\ddagger}{}_{cent}$[c]	G2(+) $\Delta H_0^{\ddagger}{}_{ovr}$[c]	$\Delta H^{\ddagger}{}_{cent}$ eq 9	$\Delta H^{\ddagger}{}_{ovr}$ eq 10	$\Delta H^{\ddagger}{}_{ovr}$ eq 11
F, Cl	−102.4	0.254 (0.235)	52.0	1.8	13.4	−42.4	−43.1
F, Br	−125.3	0.170 (0.176)	47.5	−1.1	5.5	−50.1	−49.5
F, I	−138.9	0.117 (0.139)	45.5	−0.8	2.5	−48.5	−48.3
Cl, Br	−24.8	0.439 (0.436)	51.2	8.7	39.6	−5.9	−6.2
Cl, I	−38.6	0.402 (0.400)	49.0	9.0	31.6	−12.1	−12.9
Br, I	−13.5	0.462 (0.465)	44.7	6.2	38.2	−2.3	−2.4

[a] Central enthalpy differences (kJ mol^{-1}) between the reactant and product ion−molecule complexes, **1** and **3**. [b] Calculated with eq 12 using the intrinsic barriers found with eq 8. The α values calculated with an intrinsic barrier averaged for all $Y^- + CH_3X$ reactions (Y, X = F−I) are given in parentheses. The two sets give averaged α values of 0.307 and 0.309, respectively. The α value obtained from the slope of the linear plot of $\Delta H^{\ddagger}{}_{cent}$ versus ΔH_{cent} (Figure 3) is 0.323. The G2(+) averaged intrinsic barrier for reaction 2 is 48.3 kJ mol^{-1} (at 0 K). [c] Calculated using eq 8 from the G2(+) data on the identity methyl-transfer reaction 1.[9]

Polanyi:[75b]

$$\Delta H^{\ddagger} = \alpha \Delta H + C \qquad (6)$$

which relates the enthalpy of activation ($\Delta H^{\ddagger}$) to the reaction enthalpy (ΔH) for a reaction family.[76]

A further interesting feature of the non-identity S_N2 set is an excellent correlation ($r^2 = 1.000$) between the overall reaction enthalpy (ΔH_{ovr}) and the enthalpy difference between product and reactant ion−molecule complexes (ΔH_{cent}). This correlation is observed despite substantial differences in the reactant and product complexation enthalpies.

A more recent barrier-height−reaction enthalpy relationship, which reduces to the Evans−Polanyi expression over a limited reactivity range, is the Marcus equation:[20,21]

$$\Delta H^{\ddagger} = \Delta H_0^{\ddagger} + 0.5\Delta H + (\Delta H)^2/(16\Delta H_0^{\ddagger}) \qquad (7)$$

The Marcus approach treats the barrier height, $\Delta H^{\ddagger}$, as being made up of two components: an intrinsic or kinetic component, defined by the intrinsic barrier $\Delta H_0^{\ddagger}$ (which is the barrier height in the absence of a thermodynamic driving force), and a component which is due to the effect of reaction thermodynamics, ΔH. The intrinsic barrier for a non-identity reaction $Y^- + CH_3X$, $\Delta H_0^{\ddagger}{}_{(XY)}$, is estimated using the additivity postulate:[20]

$$\Delta H_0^{\ddagger}{}_{(XY)} = 0.5[\Delta H_0^{\ddagger}{}_{(XX)} + \Delta H_0^{\ddagger}{}_{(YY)}] \qquad (8)$$

where $\Delta H_0^{\ddagger}{}_{(XX)}$ and $\Delta H_0^{\ddagger}{}_{(YY)}$ are the barriers in the corresponding identity reactions, $X^- + CH_3X \rightarrow XCH_3 + X^-$ and $Y^- + CH_3Y \rightarrow YCH_3 + Y^-$, respectively. In recent years the Marcus treatment has been successfully applied to gas-phase methyl-transfer reactions in both experimental[3k,15a] and computational[2a,4j,6c,77] studies.

Given the large data set that is available from our calculations, it is of interest to test whether the Marcus treatment is applicable at the G2(+) level of theory. Since the Marcus equation is normally applied to an elementary reaction step,[20] let us first test the Marcus approach for the conversion of reactant ion−molecule complex **1** to product ion−molecule complex **3**. Accordingly, we need to compare the $\Delta H^{\ddagger}{}_{cent}$ values obtained by substituting into the Marcus equation:

$$\Delta H^{\ddagger}{}_{cent} = \Delta H_0^{\ddagger}{}_{cent} + 0.5\Delta H_{cent} + (\Delta H_{cent})^2/(16\Delta H_0^{\ddagger}{}_{cent}) \qquad (9)$$

and which are listed in Table 7 with the directly computed 0 K G2(+) $\Delta H^{\ddagger}{}_{cent}$ values of Table 3. We can see that the Marcus estimates of $\Delta H^{\ddagger}{}_{cent}$ (eq 9) are close to the calculated values (the largest difference being 2.4 kJ mol^{-1}), justifying the use of the Marcus equation for this purpose. A plot of the two data sets gives a correlation coefficient r^2 of 0.999. This agreement between the predictions of the Marcus equation and direct calculation or experimental measurement has been noted previously,[3k,15a] though many of the experimental and theoretical values on which the earlier assessments were carried out have been superseded.

In order to apply the Marcus equation to a double-well reaction profile and the overall barrier (rather than the central barrier), some modification of the equation is necessary. Such an exercise is desirable, however, since the property that is measured experimentally in a gas-phase S_N2 reaction is the overall barrier, rather than the central barrier. Accordingly, modifications of eq 7 have been proposed by Wolfe, Mitchell, and Schlegel[77] and by Dodd and Brauman.[15b]

The Wolfe, Mitchell, and Schlegel modification[77] is

$$\Delta H^{\ddagger}{}_{ovr} \approx \Delta H_0^{\ddagger}{}_{ovr} + 0.5\Delta H_{ovr} + (\Delta H_{ovr})^2/16\Delta H_0^{\ddagger}{}_{cent} \qquad (10)$$

where $\Delta H_0^{\ddagger}{}_{ovr}$ is obtained from $\Delta H^{\ddagger}{}_{ovr(XX)}$ and $\Delta H^{\ddagger}{}_{ovr(YY)}$, the overall barriers in the corresponding identity reactions, by using eq 8, and ΔH_{ovr} is now the *overall* reaction enthalpy, i.e. the enthalpy difference between products and reactants rather than between product and reactant ion−molecule complexes ΔH_{cent}. The derivation of this expression assumes (i) that the pre-reaction and post-reaction complexation enthalpies in the non-identity S_N2 reaction are equal, i.e. $\Delta H_{cent} = \Delta H_{ovr}$, and (ii) that the sum of the pre-reaction and post-reaction complexation enthalpies in the non-identity S_N2 reaction can be approximated by the sum of the complexation enthalpies of the two corresponding identity reactions.

Dodd and Brauman[15b] suggested a slightly different modification of eq 7:

$$\Delta H^{\ddagger}{}_{ovr} \approx \Delta H_0^{\ddagger}{}_{ovr} + 0.5\Delta H_{ovr} + (\Delta H_{ovr})^2/[16(\Delta H_0^{\ddagger}{}_{ovr} - \Delta H_{comp})] \qquad (11)$$

in which the term $\Delta H_0^{\ddagger}{}_{cent}$ is replaced by $(\Delta H_0^{\ddagger}{}_{ovr} - \Delta H_{comp})$. This equation may also be derived by assuming that pre-reaction and post-reaction complexation enthalpies in the non-identity S_N2 reaction are equal so that an average value of the complexation enthalpy is used for ΔH_{comp}.

(75) (a) Bell, R. P. *Proc. R. Soc. London* **1936**, *154A*, 414. (b) Evans, M. G.; Polanyi, M. *Trans. Faraday Soc.* **1938**, *34*, 11.

(76) For example, $\alpha = 0.323$ and $C = 44.7$ when $\Delta H^{\ddagger}{}_{cent}$ and ΔH_{cent} are in kJ mol^{-1} (Table 7), with $r^2 = 0.991$.

(77) Wolfe, S.; Mitchell, D. J.; Schlegel, H. B. *J. Am. Chem. Soc.* **1981**, *103*, 7694.

(78) For a discussion of Brønsted coefficients, see, for example: Bordwell, F. G.; Cripe, T. A.; Hughes, D. L. In *Nucleophilicity*; Harris, J. M., McManus, S. P., Eds.; American Chemical Society: Washington, 1987; p 137.

Inspection of the results in Table 7 shows that the Wolfe et al. (eq 10) and Dodd and Brauman (eq 11) modifications to the Marcus equation lead to very similar predictions for $\Delta H^{\ddagger}_{ovr}$. Comparison of these values with the computed G2(+) values (Table 3) indicates good estimates of $\Delta H^{\ddagger}_{ovr}$ for the three reactions where the exothermicity is small (Cl, Br; Cl, I; Br, I). Here the Marcus estimates and the calculated G2 value differ by less than 2 kJ mol^{-1}. However, for the set of reactions where the exothermicity is large, $\Delta H^{\ddagger}_{ovr}$ is significantly overestimated (by up to 20 kJ mol^{-1}). Our results suggest therefore that extension of the Marcus treatment to the overall reaction is much less reliable than its application to an elementary step, and that deviations manifest themselves primarily in strongly exothermic reactions.

Since the Marcus equation provides a good estimate of the central barrier, let us now extend the Marcus treatment to consideration of the Brønsted coefficient, α.[78] Differentiation of the Marcus equation (eq 7) with respect to ΔH and assuming $\Delta H_0^{\ddagger}$ to be constant leads[20a] to an expression for α in terms of the intrinsic barrier and the reaction enthalpy. Thus:

$$\alpha = \partial\Delta H^{\ddagger}/\partial\Delta H = 0.5 + \Delta H/(8\Delta H_0^{\ddagger}) \qquad (12)$$

The α parameter may be obtained for an individual reaction by substituting appropriate ΔH_{cent} and $\Delta H_0^{\ddagger}{}_{cent}$ values (listed in Table 7) into eq 12 in which case it is termed an intrinsic α value. Alternatively, a value of α may be obtained from the slope of the barrier-height−enthalpy correlation, in which case it is termed the group α value.[4j] Thus the intrinsic α value is a characteristic of a *particular* reaction while the group α value relates to the reaction series *as a whole*. Since the derivation of eq 12 assumes $\Delta H_0^{\ddagger}$ values to be constant, intrinsic α values were also calculated with a $\Delta H_0^{\ddagger}$ value averaged for all reactions 2 (48.3 kJ mol^{-1}).[9] The α values obtained in this manner differ only slightly from the intrinsic α values calculated with individual $\Delta H_0^{\ddagger}$ values (Table 7). The group α value for this reaction family, 0.323, is obtained from eq 6 (Figure 3).

The significance of the Brønsted parameter has been a subject of considerable debate over recent years. Of particular interest has been the question as to whether α can provide a reliable measure of transition state structure.[79] The current position appears to be that the use of the Brønsted parameter to estimate transition state structure is generally unreliable.[79] In particular, the assumption that a *group* α value may provide a measure of transition state structure for all members of the series is now considered to be invalid; it is increasingly clear that within a reaction family, even if that family obeys a rate−equilibrium relationship, considerable variability in the transition structure takes place.

In order to explore the mechanistic significance of the intrinsic α values (Table 7) (as opposed to the group α values), we have attempted to correlate the values with a variety of structural and energetic parameters. Excellent correlations are obtained. Thus, intrinsic α values are found to correlate with the central barriers ($r^2 = 0.984$), and since the central barriers themselves correlate well with a variety of other parameters, the intrinsic α values also correlate with the overall reaction enthalpy ($r^2 = 0.995$), with the central reaction enthalpy ($r^2 = 0.993$), with indices of the transition structure asymmetry, such as %AS‡ ($r^2 = 0.968$) and ΔWBI ($r^2 = 0.992$) (Tables 6 and 8), and with the charge distribution asymmetry in **2**, Δq(X−Y) ($r^2 = 0.956$).

The ability of the intrinsic α values to correlate with reaction enthalpy and with transition structure asymmetry reaffirms that S_N2 reactivity, at least for the halide-exchange reaction, conforms to the Marcus reactivity pattern. Thus, in the present case the intrinsic α values do provide at least a *relative* measure of transition state structure, and the more exothermic reactions do have earlier transition states. However, it is important to appreciate that even though the present system does obey the Marcus relationships, this should not be interpreted to mean that all reaction families follow the same pattern. It is increasingly clear that the Marcus description is an idealized one and that it does not apply to all reaction families.[80]

Table 8. Linear Correlations of Various Characteristics of $Y^- + CH_3X$ Reactions (Y, X = F−I) Calculated at the G2(+) Level

entry	parameter 1	parameter 2	r^2
1	$\Delta H^{\ddagger}_{cent}$(0 K)	ΔH_{ovr}(0 K)	0.991
2	$\Delta H^{\ddagger}_{cent}$(0 K)	ΔH_{cent}(0 K)	0.991
3	$\Delta H^{\ddagger}_{cent}$(0 K)	$\Delta H^{\ddagger}_{cent}$(Marcus, eq 9)	0.999
4	$\Delta H^{\ddagger}_{cent}$(0 K)	Δq(X−Y)	0.912
5	$\Delta H^{\ddagger}_{cent}$(0 K)	%L‡	0.821
6	$\Delta H^{\ddagger}_{cent}$(0 K)	%AS‡	0.922
7	$\Delta H^{\ddagger}_{ovr}$(0 K)	$\Delta H^{\ddagger}_{ovr}$(Marcus, eq 10)	0.994
8	$\Delta H^{\ddagger}_{ovr}$(0 K)	$\Delta H^{\ddagger}_{ovr}$(Marcus, eq 11)	0.990
9	$\Delta H^{\ddagger}_{ovr}$(0 K)	ΔH_{ovr}(0 K)	0.995
10	α	$\Delta H^{\ddagger}_{cent}$(0 K)	0.984
11	α	ΔH_{cent}(0 K)	0.993
12	α	ΔH_{ovr}(0 K)	0.995
13	α	%AS‡	0.968
14	α	ΔWBI	0.992
15	α	Δq(X−Y)	0.956
16	Δq(X−Y)	%AS‡	0.995
17	Δq(X−Y)	ΔWBI	0.957
18	ΔH_{ovr}(0 K)	ΔH_{cent}(0 K)	1.000
19	ΔH_{ovr}(298 K)	%L‡	0.882
20	ΔH_{ovr}(298 K)	%AS‡	0.944
21	ΔH_{ovr}(298 K)	Δq(X−Y)	0.927
22	ΔH_{ovr}(298 K)	ΔWBI	0.990

2. Correlation of the Central Barriers. Both the central barrier and overall barrier in reaction 2 correlate with the reaction enthalpy ($r^2 = 0.991$ and 0.995, respectively, Table 8). The latter is consistent with the experimental observation that S_N2 rate constants and reaction efficiencies increase as the reaction exothermicity increases.[3c,k,l,18,49,54,64] Furthermore, as observed for the identity methyl-transfer reactions 1,[9] we find a reasonable correlation between the central barrier heights and the looseness of the transition structure, %L‡ [81] ($r^2 = 0.821$, Table 8 and Figure 4). Central barrier heights are also found to correlate with the geometrical asymmetry of the transition structure, %AS‡, and the charge distribution asymmetry, Δq(X−Y) ($r^2 = 0.922$ and 0.912, respectively). Taken together these correlations provide further evidence for the Marcus reactivity pattern.

Of special interest is the observation that the geometrical asymmetry of the transition structure **2**, %AS‡, exhibits a good correlation with the charge asymmetry of **2**, q(X−Y) ($r^2 =$

(79) Pross, A.; Shaik, S. *New J. Chem.* **1989**, *13*, 427 and references therein.

(80) For example, radical addition to alkenes does not obey the simple Marcus formulation. For details, see: Wong, M. W.; Pross, A.; Radom, L. *J. Am. Chem. Soc.* **1994**, *116*, 6284.

(81) We should mention that calculations of the %CX‡ index, modified[8,82] by taking the C−X bond lengths in the reactant geometry rather than the bond lengths in the reactant ion−molecule complex as suggested originally,[66] can give rise to different results. For example, while there is a reasonable correlation ($r^2 = 0.939$) between G2(+) $\Delta H^{\ddagger}_{cent}$ and %CX‡ values in reaction 1 when %CX‡ is calculated from the C−X bond length in the reactant ion−molecule complex geometry,[9] such a correlation is evidently lacking or is quite poor ($r^2 = 0.659$) for reaction 1 if the %CX‡ index is found using the reactant C−X bond lengths. These results do not support the generality of the conclusion[8] that the difference between these two definitions of the transition structure looseness is negligible.

(82) Lee, I.; Kim, C. K.; Chung, D. S.; Lee, B.-S. *J. Org. Chem.* **1994**, *59*, 4490.

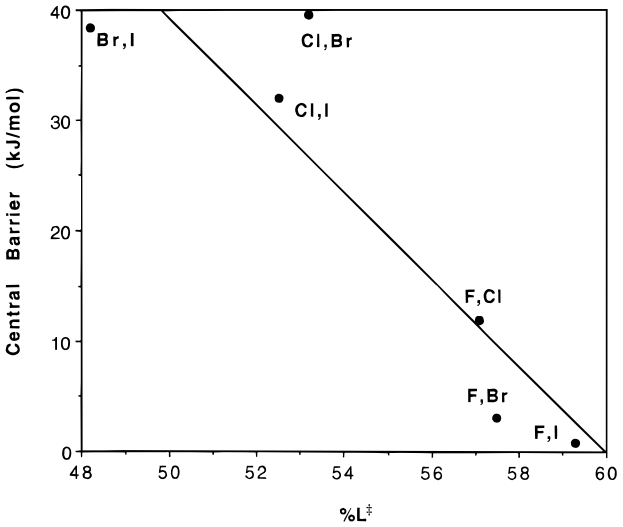

Figure 4. Plot of the G2(+) central barriers ($\Delta H^{\ddagger}_{cent}$) vs the geometric looseness index of transition structures **2** (%L‡) for the $Y^- + CH_3X$ non-identity exchange reactions (Y, X = F−I) at 0 K (see eqs 4a−c). The MP2/6-31+G(d) values of %L‡ as well as of its components, %CX‡ and %CY‡, are presented in Table 5.

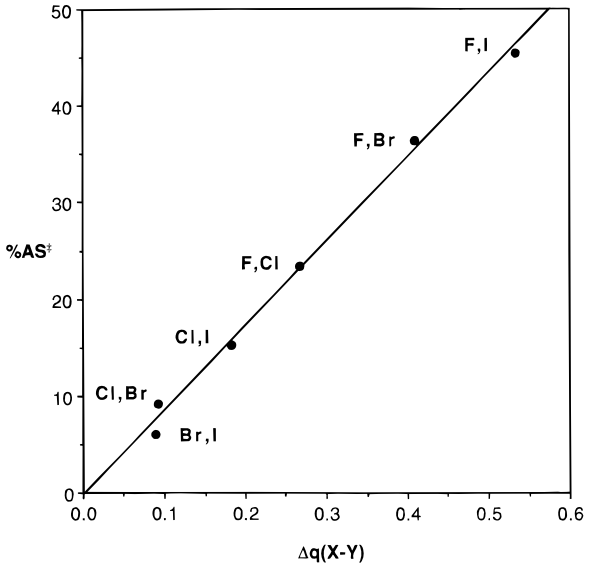

Figure 5. Plot of the geometric asymmetry index (%AS‡) vs the charge asymmetry index (Δq(X−Y)) in transition structures **2** for the $Y^- + CH_3X$ non-identity exchange reactions (X, Y = F−I). Indexes (%AS‡) and Δq(X−Y) are listed in Tables 5 and 6, respectively.

0.998) (Figure 5). In other words, early transition states in a geometric sense are also early in a charge sense. While this pattern might be expected from the Leffler postulate[83] which implies that the charge and geometric progression of the reaction coordinate proceed more or less in tandem, a theoretical analysis, based on curve-crossing considerations, suggests that this view is simplistic,[84] and that charge and geometric progression are not necessarily simply related. The curve-crossing model indicates that the electronic character of the transition state is governed by the nature and mix of the electronic configurations that contribute to the transition state electronic wave function, located at the crossing point of reactant and product configurations,[84] rather than by the geometric "earliness" or "lateness" of the transition structure.

(83) (a) Leffler, J. E. *Science* **1953**, *117*, 340. (b) Leffler, J. E.; Grunwald, E. *Rates and Equilibria in Organic Reactions;* Wiley: New York, 1963.
(84) Pross, A.; Shaik, S. *Croat. Chem. Acta* **1992**, *65*, 625.

Table 9. G2(+) Calculated Index ($T^{\ddagger}$) of Thermochemical Looseness of the YCH_3X^- Transition Structures (**2**, Y, X = F, Cl, Br, and I)

species	$\Delta H^{\ddagger}_{ovr(f)}$[a]	$\Delta H^{\ddagger}_{ovr(r)}$[a]	ΔIE[b]	$D_{C-X} + D_{C-Y}$[c]	$T^{\ddagger}$[d]
F···CH_3···Cl^- (**2a**)	−54.7	75.0	11.9	810.3	0.96
F···CH_3···Br^- (**2a**)	−67.7	93.8	17.4	748.5	0.94
F···CH_3···I^- (**2a**)	−68.8	108.9	48.5	700.2	0.87
Cl···CH_3···Br^- (**2a**)	−15.3	25.3	29.2	632.8	0.93
Cl···CH_3···I^- (**2a**)	−3.5	36.2	60.4	584.5	0.86
Br···CH_3···I^- (**2a**)	−8.0	15.6	31.2	522.7	0.92

[a] $\Delta H^{\ddagger}_{ovr(f)}$ and $\Delta H^{\ddagger}_{ovr(r)}$ are G2(+) overall barriers (in kJ mol^{-1}) of the forward and reverse reactions, respectively, of eq 2. [b] G2(+) ionization energies (IE) of the halide anions are taken from ref 9. [c] G2(+) dissociation energies (D_{C-X}, 0 K) of the C−X bond in CH_3X (X = F−I) are taken from ref 85. [d] Defined by eq 13.

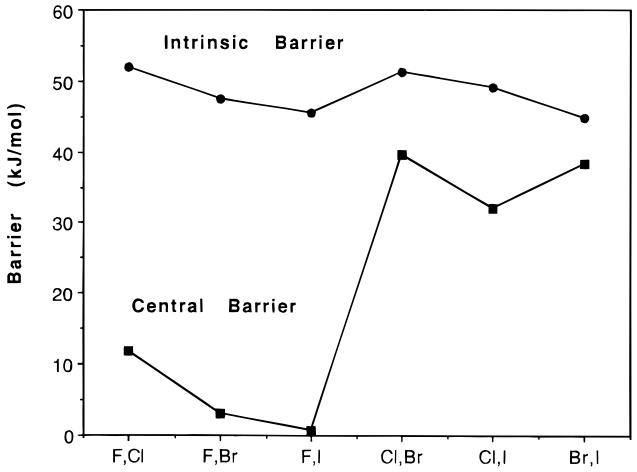

Figure 6. Trends in the central barriers ($\Delta H^{\ddagger}_{cent}$) and intrinsic central barriers ($\Delta H_0^{\ddagger}{}_{cent}$) for the $Y^- + CH_3X$ non-identity exchange reaction (Y, X = F−I) at 0 K. Values of $\Delta H^{\ddagger}_{cent}$ and $\Delta H_0^{\ddagger}{}_{cent}$ are listed in Tables 3 and 7, respectively.

On this basis the observed correlation between geometric asymmetry and charge asymmetry is surprising. One possible phenomenon that may account for the charge−geometry correlation is curve skewing,[84] which would lead to the prediction that highly exothermic reactions are likely to have their transition states appearing at an earlier geometry than that defined by the crossing point of reactant and product configurations. As a consequence, the contribution of the reactant configuration to the electronic structure of the transition state increases, leading to a transition state that is early not just in a geometric sense but in a charge sense as well. This point will need to be further clarified.

Finally, we find no correlation between the central barrier or the sum of the forward and reverse overall barriers with the index of thermochemical looseness of the transition structure, $T^{\ddagger}$, defined by eq 12 (whose values are listed in Table 9), as suggested recently:[73]

$$T^{\ddagger} = 1 - (\Delta H^{\ddagger}_{ovr(f)} + \Delta H^{\ddagger}_{ovr(r)} + |\Delta IE_{XY}|)/(D_{C-X} + D_{C-Y}) \quad (13)$$

3. Correlation of the Intrinsic Barriers. The trends in the central and intrinsic (central) barriers for reaction 2 are shown in Figure 6. As would be expected, the intrinsic barriers show only slight variation for different systems, compared with the central barriers which vary markedly. Furthermore, in accord with the prediction of the Marcus equation, it can be seen that the more exothermic the reaction, the greater the difference in these energies.

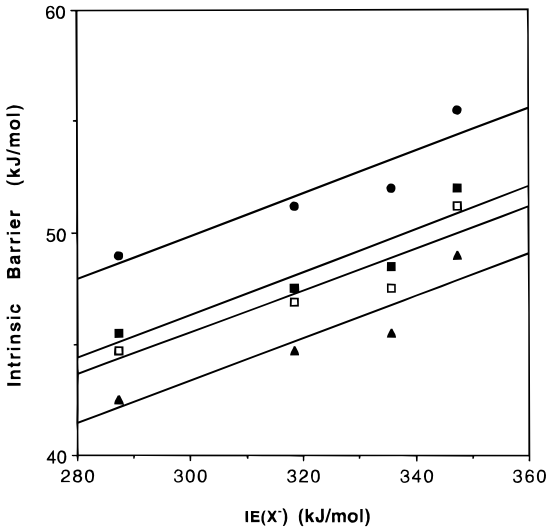

Figure 7. Plot of the G2(+) intrinsic central barriers ($\Delta H_0^{\ddagger}_{cent}$, 0 K) vs the G2(+) gas-phase ionization energies of X^- ($IE(X^-)$) in the reaction series $Y^- + CH_3X$ where Y = F−I and X = F (■), Cl (●), Br (□), and I (▲). The G2(+) values of $\Delta H_0^{\ddagger}_{cent}$ for non-identity reactions are listed in Table 7 while the $\Delta H_0^{\ddagger}_{cent}$ values for identity reactions and the $IE(X^-)$ values are taken from ref 9.

It has been suggested that a combination of strong C−Y and C−X bonds and low ionization energies of Y^- and X^- should cause high intrinsic barriers in non-identity S_N2 reactions.[2a] However, we do not find any correlation of the intrinsic barriers with the sum or the difference in the C−Y and C−X bond energies. For example, within the set $Cl^- + CH_3X$ (X = F, Cl, Br, and I), the correlation between the intrinsic barrier and the C−X bond dissociation energy, D_{C-X}, breaks down for X = F. Moreover, we have found that the intrinsic barriers show reasonable linear correlations with the ionization energies of Y^- in the reaction series. $Y^- + CH_3X$ ($r^2 = 0.851$ for $Y^- + CH_3F$ (Y= F−I), $r^2 = 0.857$ for $Y^- + CH_3Cl$ (Y = F−I), $r^2 = 0.834$ for $Y^- + CH_3Br$ (Y = F−I), $r^2 = 0.857$ for $Y^- + CH_3I$ (Y = F−I)) rather than inverse correlations (Figure 7). Analogous correlations between the intrinsic barrier and the ionization energies of halide anions have been found for the identity reactions at saturated carbon and nitrogen.[9,85]

According to the curve-crossing model, the intrinsic barrier in both identity and non-identity S_N2 reactions and the central barrier in a non-identity S_N2 reaction are likely to be greatly influenced by the initial energy gap between reactant and product configurations, $IE(X^-) - EA(RX)$, where $IE(X^-)$ and EA(RX) are gas-phase ionization energies of X^- and gas-phase vertical electron affinities of RX, respectively.[2a] This suggests that intrinsic barriers could in some circumstances correlate with $IE(X^-) - EA(RX)$. Unfortunately, as we have already noted previously,[9] the available experimental[86] and theoretical data[87] on the vertical gas-phase electron affinities of the methyl halides vary widely, making the testing of this idea problematic. We have therefore not attempted to check for such a correlation.

4. Correlation of Reaction Enthalpy with Characteristics of the Transition Structures. The existence of a correlation between the α coefficient and reaction enthalpy, ΔH_{ovr}, implies that the reaction enthalpy correlates with the various indices of transition structure asymmetry. The data in Table 8 list such correlations with, for example, geometrical asymmetry, $\%AS^{\ddagger}$ ($r^2 = 0.944$), bonding asymmetry, ΔWBI ($r^2 = 0.990$), and charge asymmetry, $\Delta q(X-Y)$ ($r^2 = 0.927$). In turn, these indexes also correlate with one another.

Conclusions

Application of G2(+) theory to the non-identity S_N2 reactions of halide anions with methyl halides, $Y^- + CH_3X \rightarrow YCH_3 + X^-$ (Y, X = F, Cl, Br, and I), leads to the following conclusions.

(1) Central barrier heights ($\Delta H^{\ddagger}_{cent}$) vary from 0.8 kJ mol^{-1} for the reaction $F^- + CH_3I$ to 39.5 kJ mol^{-1} for the reaction $Cl^- + CH_3Br$ (at 0 K). These central barriers are lower than those in the identity S_N2 reactions $X^- + CH_3X$ and the lowering is attributed to the effect of reaction exothermicity which ranges from −177.5 kJ mol^{-1} for $F^- + CH_3I$ to −17.9 kJ mol^{-1} for $Br^- + CH_3I$. The central barriers demonstrate a good linear correlation with overall reaction exothermicity (ΔH_{ovr}) as well as with the central exothermicity (ΔH_{cent}), as measured from reactant ion−molecule complex to product ion−molecule complex.

(2) Overall barriers for all exothermic $Y^- + CH_3X$ reactions are found to be negative, in contrast to those for the identity reactions $X^- + CH_3X$, where only the barrier for X = F is negative. Values vary from −68.8 (for $F^- + CH_3I$) to −2.3 kJ mol^{-1} (for $Br^- + CH_3I$). Overall barriers also demonstrate a good linear correlation with the reaction exothermicity.

(3) The G2(+) central and overall barriers for the reaction of $Cl^- + CH_3Br$ agree with currently available experimental data. However, the calculated central barrier for $F^- + CH_3Cl$ (9.9 kJ mol^{-1}) is significantly lower than the experimentally determined value (29 kJ mol^{-1}). The possible importance of non-statistical effects in the evaluation of experimental barrier heights needs to be evaluated. In any case, the high level of electron correlation and large basis sets employed in G2(+) theory are concluded to be essential in obtaining reliable barrier heights computationally.

(4) Complexation enthalpies (ΔH_{comp}) of ion−molecule complexes $Y^-\cdots CH_3X$ at 298 K increase from 30.4 kJ mol^{-1} for Y = F, X = I to 69.5 kJ mol^{-1} for Y = I, X = F, and are in good agreement with experimental and earlier computational studies. Complexation enthalpies for $Y^-\cdots CH_3X$ involving a particular CH_3X are found to exhibit good linear correlations with the electronegativity of Y.

(5) The set of non-identity S_N2 reactions obeys both the Evans−Polanyi barrier-height−enthalpy (rate−equilibrium) relationship and the Marcus equation. Thus, central barriers estimated from the Marcus equation show a good correlation with the directly calculated central barriers. Modifications of the Marcus equation used to estimate overall barriers are found to be less reliable and give reasonable results only in those cases where reaction exothermicity is small.

(6) Intrinsic α values (eq 12) for each reaction are found to correlate with reaction enthalpy, geometrical looseness ($\%L^{\ddagger}$), geometrical asymmetry ($\%AS^{\ddagger}$), charge asymmetry ($\Delta q(X-Y)$), and bond asymmetry (ΔWBI) of the transition structures, indicating that gas-phase S_N2 reactions for halide exchange are well described by Marcus theory. Accordingly, the Leffler idea

(85) Glukhovtsev, M. N.; Pross, A.; Radom, L. *J. Am. Chem. Soc.* **1995**, *117*, 9012.

(86) (a) Giordan, J. C.; Moore, J. H.; Tossell, J. A. *Acc. Chem. Res.* **1986**, *19*, 281. (b) Jordan, K. D.; Burrow, P. D. *Chem. Rev.* **1987**, *87*, 557. (c) Benitez, A.; Moore, J. H.; Tossell, J. A. *J. Chem. Phys.* **1988**, *88*, 6691. (d) Modelli, A.; Scagnolari, F.; Distefano, G.; Jones, D.; Guerra, M. *J. Chem. Phys.* **1992**, *96*, 2061. (e) Krzysztofowicz, A. M.; Szmytkowski, C. *Chem. Phys. Lett.* **1994**, *219*, 86.

(87) Calculations of negative electron affinities are complicated by obtaining solutions which correspond to the neutral molecule plus a free electron rather than to the anion. For details, see (a) Guerra, M. *Chem. Phys. Lett.* **1990**, *167*, 315. (b) Simons, J.; Jordan, K. D. *Chem. Rev.* **1987**, *87*, 535. (c) Bertran, J.; Gallardo, I.; Moreno, M.; Savéant, J.-M. *J. Am. Chem. Soc.* **1992**, *114*, 9576. (d) Heinrich, N.; Koch, W.; Frenking, G. *Chem. Phys. Lett.* **1986**, *124*, 20. (e) Kalcher, J.; Sax, A. F. *Chem. Rev.* **1994**, *94*, 2291.

that more exothermic reactions have earlier transition states is shown to be valid for the above reaction set.

(7) G2(+) central barriers, $\Delta H^{\ddagger}_{cent}$, and overall reaction enthalpies, ΔH_{ovr}, exhibit good linear correlations with the geometric looseness ($\%L^{\ddagger}$), geometric asymmetry ($\%AS^{\ddagger}$), charge asymmetry ($\Delta q(X-Y)$), and bond asymmetry (ΔWBI) of the transition structures. Neither the central barrier nor the overall barrier correlate with the thermochemical looseness parameter ($T^{\ddagger}$).

Acknowledgment. We gratefully acknowledge a generous allocation of time on the Fujitsu VP−2200 computer of the Australian National University Supercomputer Facility, the support of the Australian Research Council, and the award (to A.P.) of an ARC Senior Research Fellowship, and we thank Professor Don Truhlar for providing us with a preprint of ref 7.

Supporting Information Available: Calculated G2(+) total energies for species involved in the non-identity reaction of Y- with CH_3X (Table S1), and plot of the G2(+) complexation enthalpies (ΔH_{comp}, 298 K) of the ion−molecule complexes $Y^{-}\cdots CH_3X$ vs Mulliken electronegativities of the halogens (Figure S1) (3 pages). This material is contained in many libraries on microfiche, immediately follows this article in the microfilm version of the journal, can be ordered from the ACS, and can be downloaded from the Internet; see any current masthead page for ordering information and Internet access instructions.

JA953665N